Journal of the American Heart Association

ORIGINAL RESEARCH

Sodium Glucose Transporter 2 Inhibitor Protects Against Heart Failure With Preserved Ejection Fraction: Preclinical "2-Hit" Model Reveals Autophagy Enhancement Via AMP-Activated Protein Kinase/Mammalian Target of Rapamycin Complex 1 Pathway

Xinyu Hu, MD*; Dan Li, PhD*; Weijie Chen, MD; Hongyu Kuang, MD; Dan Yang, PhD; Zhiyan Gong, MD; Yuxiang Long, MD; Guangliang Liu, PhD; Kai Wang, MD; Mengshi Xia, MD; Yanping Xu, MD†; Yuehui Yin, MD†

BACKGROUND: Heart failure with preserved ejection fraction (HFpEF) is a multifaceted syndrome with high morbidity and mortality. Empagliflozin, an SGLT2 (sodium–glucose cotransporter 2) inhibitor, reduces adverse events in patients with HFpEF regardless of glycemic control. However, the precise cardioprotective mechanisms of SGLT2 inhibitor in HFpEF remain underexplored.

METHODS AND RESULTS: A "2-hit" mouse model of HFpEF was developed via the high-fat diet combined with N^{ω}-nitro-L-arginine methyl ester. Male C57BL/6N mice were assigned to either a control group (n=10) or an HFpEF group (n=20), with the latter receiving empagliflozin (10 mg/kg per day, n=10) or vehicle (n=10) for 8 weeks. Cardiac function, hypertrophy, and fibrosis were evaluated by physiological, biochemical, and histological measurements. Mechanistic analysis, including RNA sequencing, Western blotting, and immunohistochemistry, was conducted. In vitro, H9c2 cardiomyocytes were exposed to angiotensin II and palmitate, followed by empagliflozin treatment. In vivo, empagliflozin treatment improved body weight, blood pressure, glucose tolerance, and reduced cardiac hypertrophy, fibrosis, and diastolic dysfunction in HFpEF mice. Mechanistic analysis revealed that empagliflozin modulated the AMPK (AMP-activated protein kinase)/mTORC1 (mammalian target of rapamycin complex 1)/autophagy signaling pathway. Specifically, empagliflozin restored the autophagy markers (Beclin1 and LC3-II [microtubule-associated protein 1 light chain 3]) and altered the phosphorylation of AMPK, mTOR, and p70S6K (ribosomal protein S6 kinase beta-1). Inhibition of AMPK or autophagy nullified the antihypertrophic effect of empagliflozin, underscoring the dependence on the AMPK/mTORC1/autophagy pathway.

CONCLUSIONS: Empagliflozin effectively ameliorates cardiac remodeling and diastolic dysfunction in HFpEF by enhancing autophagy via the AMPK/mTORC1 pathway. These findings elucidate the direct cardioprotective mechanisms of empagliflozin and suggest potential therapeutic molecular targets for HFpEF.

Correspondence to: Yanping Xu, MD and Yuehui Yin, MD, Department of Cardiovascular Medicine, The Second Affiliated Hospital of Chongqing Medical University, No. 288 Tianwen Avenue, Nan'an District, Chongqing 400072, China. Email: xuyanping@cqmu.edu.cn; yinyh@hospital.cqmu.edu.cn

*Xinyu Hu and Dan Li contributed equally as co-first authors.

†Yanping Xu and Yuehui Yin contributed equally as co-corresponding authors.

This article was sent to Sakima Ahmad Smith, MD, MPH, Associate Editor, for review by expert referees, editorial decision, and final disposition.

Supplemental Material is available at https://www.ahajournals.org/doi/suppl/10.1161/JAHA.124.040093

For Sources of Funding and Disclosures, see page 20.

JAHA is available at: www.ahajournals.org/journal/jaha

Key Words: autophagy ■ cardiac remodeling ■ diastolic function ■ HFpEF ■ SGLT2 inhibitor

RESEARCH PERSPECTIVE

What Is New?

- Empagliflozin significantly improves heart failure with preserved ejection fraction status in a preclinical "2-hit" model.
- The cardioprotective effects of empagliflozin are linked to autophagy via the AMPK (AMP-activated protein kinase)/mTORC1 (mammalian target of rapamycin complex 1) pathway.
- This study highlights the molecular mechanisms of empagliflozin as a cardiometabolic therapy for heart failure with preserved ejection fraction.

What Question Should Be Addressed Next?

- Future studies should elucidate the antifibrotic remodeling mechanisms induced by SGLT2 (sodium-glucose cotransporter 2) inhibitors in cardiometabolic heart failure with preserved ejection fraction and systematically evaluate the therapeutic potential of AMPK agonists and autophagy modulators in heart failure with preserved ejection fraction.

Nonstandard Abbreviations and Acronyms

Ang II	angiotensin II
CCK-8	cell counting kit-8
DEGs	differentially expressed genes
HFpEF	heart failure with preserved ejection fraction
SGLT2	sodium-glucose cotransporter 2
SGLT2i	sodium-glucose cotransporter 2 inhibitor

Heart failure with preserved ejection fraction (HFpEF) is a multifaceted syndrome that primarily arises from severe obesity, diabetes, hypertensive cardiac hypertrophy, and associated comorbidities. Affecting more than 13 million adults worldwide, with its prevalence increasing by approximately 10% per decade, HFpEF has become a challenging pandemic in contemporary cardiology.[1] Characterized by diastolic dysfunction due to impaired left ventricular (LV) relaxation or increased ventricular stiffness, HFpEF is accompanied by cellular alterations and structural cardiac remodeling, including inflammation, cardiomyocyte hypertrophy, and fibrosis.[2] This condition ultimately leads to decreased relaxation of the left ventricle despite the contractile capacity remaining within the normal range.

Although the substantial morbidity and mortality in HFpEF are comparable to those in HF with reduced EF, effective treatments for HFpEF remained elusive until the EMPEROR-Preserved (Empagliflozin Outcome Trial in Patients With Chronic Heart Failure With Preserved Ejection Fraction) trial demonstrated the benefits of SGLT2 (sodium–glucose cotransporter 2) inhibitors (SGLT2is).[3] Empagliflozin, a representative SGLT2i, is an oral medication that promotes renal glucose excretion and improves glycemic control. Remarkably, in the EMPEROR-Preserved trial, empagliflozin reduced the composite risk of cardiovascular death or HF hospitalization irrespective of plasma glucose levels, suggesting cardiovascular protection beyond its hypoglycemic properties. Of note, SGLT2 receptors are rarely expressed in the heart[4] and studies have shown that SGLT2i attenuates HF in SGLT2-global-knockout mice,[5,6] indicating potential SGLT2-independent mechanisms in HFpEF that warrant further investigation. Several direct off-target mechanisms of action for SGLT2i (eg, modulation of myocardial energy metabolism, anti-inflammatory and antioxidant effects, and reversal of cardiac remodeling) are emerging as current research frontiers.[7–9] However, the precise mechanisms through which empagliflozin confers cardioprotection in HFpEF remain unclear.

Cardiac remodeling is intrinsic to the progression of diastolic dysfunction in HF and is strongly influenced by metabolic disorders.[10] The existing evidence has shown that empagliflozin ameliorates LV remodeling in both clinical trials and animal experiments of nondiabetic HF with reduced EF.[11,12] Nevertheless, research on the effects of SGLT2i on cardiac remodeling in HFpEF is limited, especially studies exploring the underlying mechanisms involved. This gap in research is partly attributable to the paucity of appropriate animal models. The pathogenesis of HFpEF is heterogeneous and involves metabolic abnormalities, neuroendocrine system activation, chronic systemic inflammation, and natriuretic peptide deficiency. Traditional single-factor preclinical models of obesity, hypertension, and diabetes fail to adequately recapitulate diverse HFpEF phenotypes.[13] Recently, a novel "2-hit" mouse model of HFpEF was established, in which a high-fat diet and N^{ω}-nitro-l-arginine methyl ester (L-NAME) were used to induce key multifactorial extracardiac and cardiac features of the disease.[14] This model offers a promising approach for investigating cardiometabolic HFpEF mechanisms and developing more effective pharmacotherapies to address clinical needs.

Therefore, this study aimed to investigate the impacts of empagliflozin on cardiac pathological remodeling and diastolic dysfunction in the well-established "2-hit" murine model of HFpEF, elucidating the underlying molecular mechanisms in combination with transcriptomic analysis.

METHODS

Data Availability

All data supporting the findings of this study are available from the corresponding authors upon reasonable request. A detailed description of all materials and methods can be found in Data S1.

Experimental Animals

This study complied with the ethical requirements of the *Guidelines for the Care and Use of Laboratory Animals* (National Institutes of Health, revised 2011) and the principles of the Declaration of Helsinki. All animal experiments were approved by the Ethical Committee of the Second Hospital of Chongqing Medical University (Approval No. 157/2022). Thirty male C57BL/6 N mice, approximately 8 weeks old, were randomly assigned to either the control group (n=10) or the HFpEF group (n=20), with allocation concealment ensured by tagging the mice. The HFpEF group was subjected to an 8-week high-fat diet (D12492, Research Diet, USA) consisting of 60% fat, 20% protein, and 20% carbohydrate combined with L-NAME (0.5 g/L, Sigma–Aldrich, USA) in their drinking water, with the pH adjusted to 7.4.[14] All the mice were maintained on a 12-hour light/dark cycle (06:00–18:00) with unrestricted access to food and water. Echocardiography was performed to assess LV function, after which the HFpEF group was randomly subdivided into HFpEF (n=10) and HFpEF plus empagliflozin treatment (HFpEF+empagliflozin, n=10) for an additional 8 weeks. The HFpEF+empagliflozin group received empagliflozin (10 mg/kg per day) via oral gavage with 0.5% hydroxyethylcellulose as the vehicle (Boehringer Ingelheim Pharma GmbH & Co., KG, Germany),[15] whereas the other groups received normal saline and vehicle. At 24 weeks of age, the mice were euthanized under sodium pentobarbital anesthesia (50 mg/kg, IP), and their hearts were excised, weighed, dissected in PBS, and stored at −80 °C. The ratios of heart weight to tibial length were also measured as a morphometric index for cardiac hypertrophy.

Tail-Cuff Blood Pressure Recordings

Resting blood pressure (BP) and heart rate were measured noninvasively in conscious mice via the tail-cuff method and system (BP-2010A; Softron Biotechnology, Beijing, China). BP was recorded every 4 weeks, with the final value determined by averaging 5 valid readings.

Intraperitoneal Glucose Tolerance Test

Intraperitoneal glucose tolerance tests were conducted by injecting glucose (2 g/kg in saline) following a 12-hour fasting period as previously described.[14] Tail blood glucose levels (mmol/L) were measured via a glucometer at baseline (0 minutes) and at 15, 30, 60, and 120 minutes post glucose administration. Mice weights from 24 hours before the intraperitoneal glucose tolerance test were used to make glucose gels to administer a dose of 2 g/kg.

Echocardiographic Assessment

All mice underwent echocardiographic measurements at baseline, in the established HFpEF model (8 weeks), and at 8 weeks after empagliflozin treatment. Quantitative analyses encompassed LV structural indices (end-diastolic diameter, wall thickness) and functional parameters, including systolic performance (ejection fraction, fractional shortening) and diastolic compliance (E/A ratio, deceleration time, and isovolumic relaxation time). Methodology is outlined and detailed in Data S1.

Serum Biochemical and Circulatory Marker Measurements

At the end of the study, fasting blood was collected via retro-orbital puncture from mice anesthetized with intraperitoneal sodium pentobarbital (50 mg/kg). Serum was separated, and biochemical and circulatory markers were measured, as outlined in Data S1.

Histological Analyses

Histopathological evaluation comprised hematoxylin and eosin staining for myofibril architecture assessment; wheat germ agglutinin staining to quantify cardiomyocyte cross-sectional area; Masson's trichrome and picrosirius red staining for collagen deposition analysis. Autophagy-related protein localization was determined through immunohistochemical detection of phospho-AMPKα (AMP-activated protein kinase alpha), phospho-mTOR (mammalian target of rapamycin), and Beclin1, combined with immunofluorescent visualization of LC3-II (microtubule-associated protein 1 light chain 3) and p62. Full methodological details are provided in Data S1.

Transmission Electron Microscopy

Fresh LV tissue was fixed, and subsequent procedures were conducted at the electron microscope facility of the Institute of Life Sciences, Chongqing Medical

University (methodology detailed in Data S1). An independent investigator examined and captured images of myocardial filament arrangement and organization, as well as the structures of mitochondria, lysosomes, autophagosomes, and autolysosomes.

Transcriptomic Analysis

RNA sequencing was performed at Shanghai Majorbio Biopharm Biotechnology Co., Ltd. (Shanghai, China). Transcriptomic analysis included Gene Ontology and Kyoto Encyclopedia of Genes and Genomes enrichment analyses of differentially expressed genes (DEGs), as well as gene set enrichment analysis. Methodology is detailed in Data S1.

Reverse Transcription Quantitative Polymerase Chain Reaction

Extraction of total RNA from the LV myocardium was performed with the Universal RNA Extraction Kit II (Accurate Biology, Hunan, China). Gene expression was normalized to β-actin expression, and changes in gene expression were calculated via the $2^{-\Delta\Delta CT}$ method. Methodology is detailed in Data S1 and the sequences of the primers used in this study are listed in Table S1.

Cell Culture

The rat embryonic cardiomyocyte cell line H9c2 was obtained from Wuhan Pricella Biotechnology Co., Ltd. The cells were cultured in DMEM (Gibco, USA) supplemented with 10% fetal bovine serum (Vazyme, Nanjing, China) and 100 U/mL penicillin/streptomycin (Beyotime, Shanghai, China) at 37 °C in 5% CO_2. Upon reaching 70% to 80% confluence, the cells were passaged by rinsing with PBS, digesting with 0.25% trypsin–EDTA, and centrifuging at 140*g* for 5 minutes before reseeding. The experiments were independently repeated at least 3 times.

Cell Counting Kit-8

Cell viability was assessed via the Cell Counting Kit-8 (CCK-8, GlpBio, USA) following standard procedures. Briefly, 5×10^3 cells were seeded in a sterile 96-well plate and incubated for 12 hours. The cells were then exposed to varying concentrations of angiotensin II (Ang II; 0.1, 1, 10, and 50 μmol/L) and palmitate (100 μmol/L) in 10% serum-DMEM for 12, 24, and 48 hours, respectively. After incubation, the medium was replaced with fresh medium, and 10 μL of CCK-8 solution was added to each well, followed by a 2-hour incubation. The absorbance was measured at 450 nm via a Thermo Varioskan LUX microplate reader (Thermo Fisher Scientific, USA). The optimal therapeutic concentration of empagliflozin (0–100 μmol/L) was determined through subsequent CCK-8 assays.

FITC-Phalloidin Staining

Phalloidin staining was used to assess morphological changes in H9c2 cells. The cells were seeded at a density of 1×10^4 cells/well in 12-well plates and exposed to 1 μmol/L AngII and 100 μmol/L palmitate for modeling or treated with 50 μmol/L empagliflozin for 24 hours. After treatment, the cells were quickly washed with PBS, fixed in 4% paraformaldehyde for 20 minutes, permeabilized with 0.1% Triton X-100 in PBS for 10 minutes, and stained with phalloidin (5 μg/mL) for 1 hour. Nuclei were counterstained with DAPI for 10 minutes at room temperature. Morphological changes were visualized with a fluorescence microscope (NIKON, ECLIPSE Ts2R, Japan) at 40× magnification. Cell size analysis was conducted via ImageJ software (National Institutes of Health, Washington, DC, USA), with approximately 200 measurements per group, on the basis of 6 random fields per dish.

Transduction of Green Fluorescent Protein-Monomeric Red Fluorescent Protein-LC3 Adenovirus

To evaluate autophagic flux and differentiate autolysosomes from autophagosomes, H9c2 cells were transduced with an adenoviral vector expressing GFP-mRFP-LC3 (green fluorescent protein-monomeric red

Figure 1. Empagliflozin improves physiological and cardiac function in the "2-hit" mouse model of HFpEF.
A, Schematic representation of the experimental design. **B**, Representative images of the mice. **C**, Statistical analysis of body weight gain and (**D**) body weight changes across the 3 groups after 8 weeks of oral gavage. **E**, Measurements of SBP, (**F**) DBP, and (**G**) HR. **H**, Results of the IPGTT and area under the curve. **I**, Representative images of transthoracic left ventricular M-mode echocardiographic tracings. **J**, Representative images of the mitral valve blood flow spectrum. **K**, Analysis of left ventricular systolic function and end-diastolic diameter in the 3 groups. **L**, Assessment of left ventricular hypertrophy parameters. **M**, Evaluation of left ventricular diastolic function via the mitral blood flow spectrum. The data are presented as mean±SEM (n=10 mice per group). Statistical analyses were conducted using 1-way ANOVA with Tukey's multiple comparison tests (**C**, **H**, **K**, **L**, **M**) and 2-way repeated measures ANOVA with Holm-Sidak post hoc tests (**D** through **G**). Statistical significance: $^*P<0.05$, $^{**}P<0.01$, $^{***}P<0.001$ vs the control group; $^{\#}P<0.05$, $^{\#\#}P<0.01$, $^{\#\#\#}P<0.001$ vs the HFpEF group. BP indicates blood pressure; BW, body weight; DBP, diastolic blood pressure; DT, deceleration time of the E peak; Echo, echocardiogram; EMPA, empagliflozin; FS, fractional shortening; HFpEF, heart failure with preserved ejection fraction; HR, heart rate; IPGTT, intraperitoneal glucose tolerance test; IVRT, isovolumetric relaxation time; IVSd, interventricular septal thickness in diastole; L-NAME, Nω-nitro-l-arginine methyl ester; LVEF, left ventricular ejection fraction; LVIDd, left ventricular internal diameter in diastole; LVPWd, left ventricular posterior wall thickness in diastole; and SBP, systolic blood pressure.

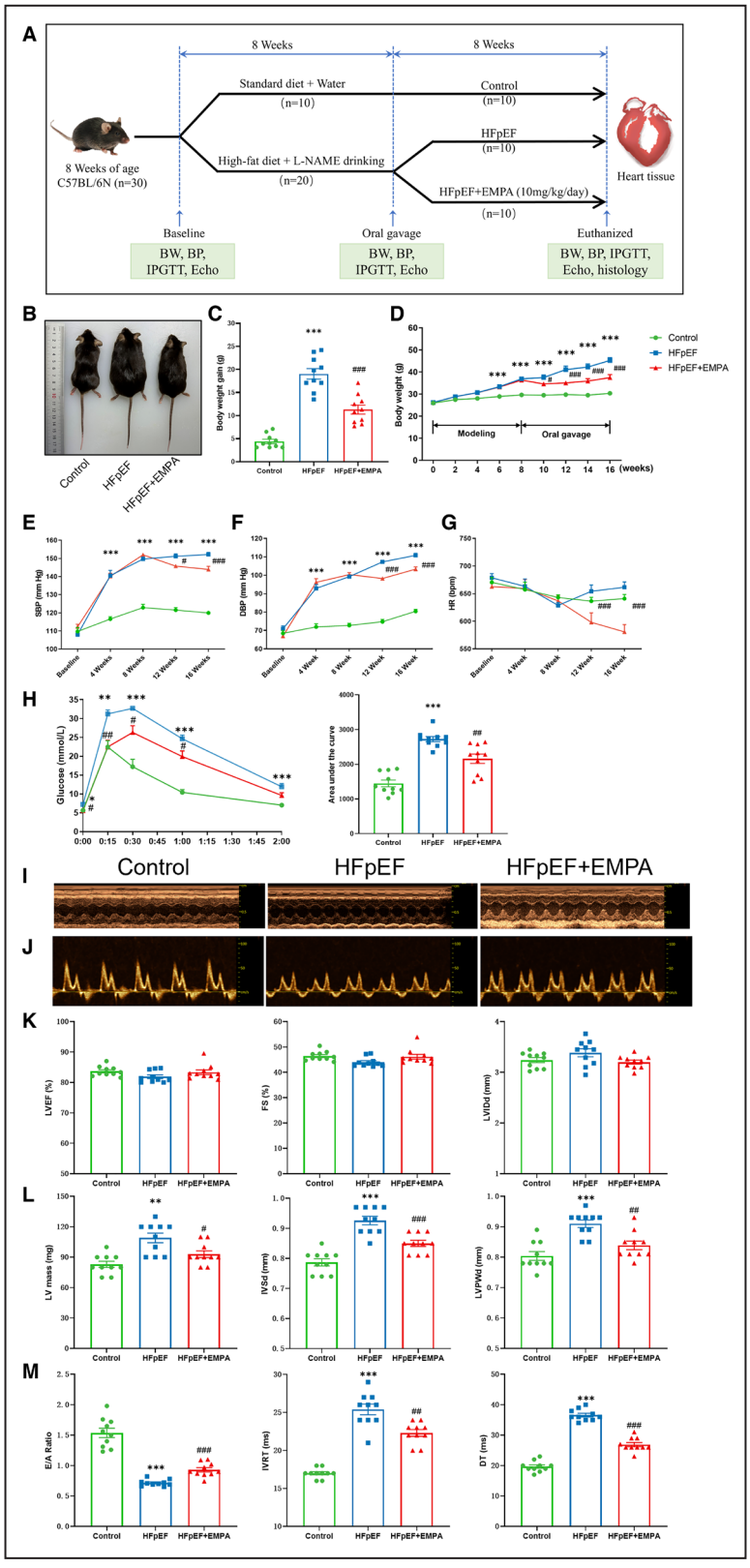

fluorescent protein-LC3; Hanbio, Shanghai, China). Cells were infected at a multiplicity of infection of 50 for 24 hours upon reaching 50% confluence. Following transduction, the cells were allocated into different experimental groups. Fluorescence images were obtained using a confocal laser scanning microscope

Table. Serum Biochemical Parameters in HFpEF Mice Treated With Vehicle or Empagliflozin

	Control	HFpEF	HFpEF+empagliflozin	*P* value
Glucose, mmol/L	7.26±0.46	12.46±1.29**	7.04±0.61##	<0.001
Insulin, mIU/L	8.75±0.52	28.18±1.33***	19.51±1.67###	<0.001
Glycated albumin, μmol/L	224.5±8.06	344.9±18.07***	246.8±6.64###	<0.001
Total cholesterol, mmol/L	2.54±0.09	6.70±0.69**	5.77±0.45	<0.001
Triglyceride, mmol/L	1.61±0.04	2.52±0.22**	2.16±0.09	<0.001
Low-density lipoprotein cholesterol, mmol/L	0.32±0.01	1.10±0.18**	0.94±0.08	<0.001
High-density lipoprotein cholesterol, mmol/L	2.47±0.13	5.98±0.57**	5.26±0.42	<0.001
Brain natriuretic peptide, pg/mL	198.70±18.09	552.10±24.05***	394.9±23.49###	<0.001
Angiotensin II, pg/mL	68.95±4.03	139.50±4.21***	102.20±7.85###	<0.001
C-reactive protein, mg/L	2.01±0.30	5.26±0.19***	3.11±0.36###	<0.001
Serum creatinine, μmol/L	22.68±2.03	26.37±3.42	28.55±1.66	0.272
Serum urea nitrogen, mg/dL	34.84±2.57	32.05±2.34	37.84±2.63	0.295

The values are means±SEMs (n=6 per group). *P* values were calculated via one-way analysis of variance, with Tukey's test used for multiple comparisons. **P*<0.05, ***P*<0.01, and ****P*<0.001 vs the control group; #*P*<0.05, ##*P*<0.01, and ###*P*<0.001 vs the HFpEF group. HFpEF indicates heart failure with preserved ejection fraction.

(Nikon, Japan). Quantitative analysis involved enumerating distinct red puncta (indicative of autolysosomes) and yellow puncta (representing autophagosomes) for subsequent evaluation.

Western Blot

Protein lysates from murine heart tissues or H9c2 cells were homogenized in RIPA buffer supplemented with protease inhibitors and a phosphate inhibitor (Beyotime, Shanghai, China) as described and detailed in Data S1.

Statistical Analysis

The experimental data are presented as mean±SEM (normally distributed) or median with interquartile range (nonnormally distributed). Statistical analyses were conducted via GraphPad Prism (v9.0). Between-group comparisons were performed with 1-way ANOVA with Tukey's post hoc (parametric, ≥3 groups) or Kruskal–Wallis with Dunn's correction (nonparametric, ≥3 groups). Repeated measures were analyzed by 2-way repeated measures ANOVA, following the assessment of sphericity. Western blot and cell viability data were normalized to the control. Statistical significance was defined as $P<0.05$.

RESULTS

Empagliflozin Improves Metabolic and Diastolic Function in HFpEF Mice

The experimental flow chart for the animal study is shown in Figure 1A. Compared with that of the control mice, the body weight of the HFpEF mice receiving a high-fat diet was significantly greater, and this difference was attenuated by empagliflozin treatment (Figure 1B through 1D). A marked increase in systolic and diastolic BP was observed in the HFpEF mice. However, empagliflozin treatment led to a significant reduction in these parameters, with systolic and diastolic BP decreasing by 8.24 mm Hg and 7.48 mm Hg, respectively (Figure 1E and 1F). Although there was no significant difference in resting heart rate between the HFpEF group and the control group, empagliflozin treatment resulted

Figure 2. Empagliflozin reduces cardiac hypertrophy and fibrosis in HFpEF mice.
A and **B**, Representative heart morphology and heart weight/tibia length ratios in control, HFpEF, and EMPA-treated HFpEF mice (n=10). **C**, Hematoxylin and eosin staining of heart sections in longitudinal and transverse views (2×, scale bar=2 mm; 400×, scale bar=50 μm). **D** and **E**, Representative WGA staining images and quantification of cardiomyocyte cross-sectional areas (n=6, scale bar=50 μm). **F** and **G**, Representative images and quantification of Masson's trichrome staining of interstitial and perivascular fibrosis in heart sections (n=6, scale bar=50 μm). **H** and **I**, Representative images and quantification of PSR staining of interstitial and perivascular fibrosis (n=6, scale bar=50 μm). **J** and **K**, RT-qPCR analysis of the mRNA levels of hypertrophic genes. **L** and **M**, RT-qPCR analysis of the mRNA levels of profibrotic genes. The data are presented as mean±SEM or median with interquartile range (TGF-β and Col-1). Statistical tests were conducted using 1-way ANOVA with Tukey's multiple comparisons (**B**, **E**, **G**, **I** through **K**) and Kruskal–Wallis tests followed by Dunn's multiple comparisons (**L**, **M**). Statistical significance: **P*<0.05, ***P*<0.01, ****P*<0.001 vs the control group; #*P*<0.05, ##*P*<0.01, ###*P*<0.001 vs the HFpEF group. β-MHC indicates beta-myosin heavy chain; Col-1, collagen type 1; EMPA, empagliflozin; H&E, hematoxylin and eosin; HFpEF, heart failure with preserved ejection fraction; HW/TL, heart weight/tibia length; PSR, picrosirius red; RT-qPCR, reverse transcription quantitative polymerase chain reaction; TGF-β, transforming growth factor-beta; and WGA, wheat germ agglutinin.

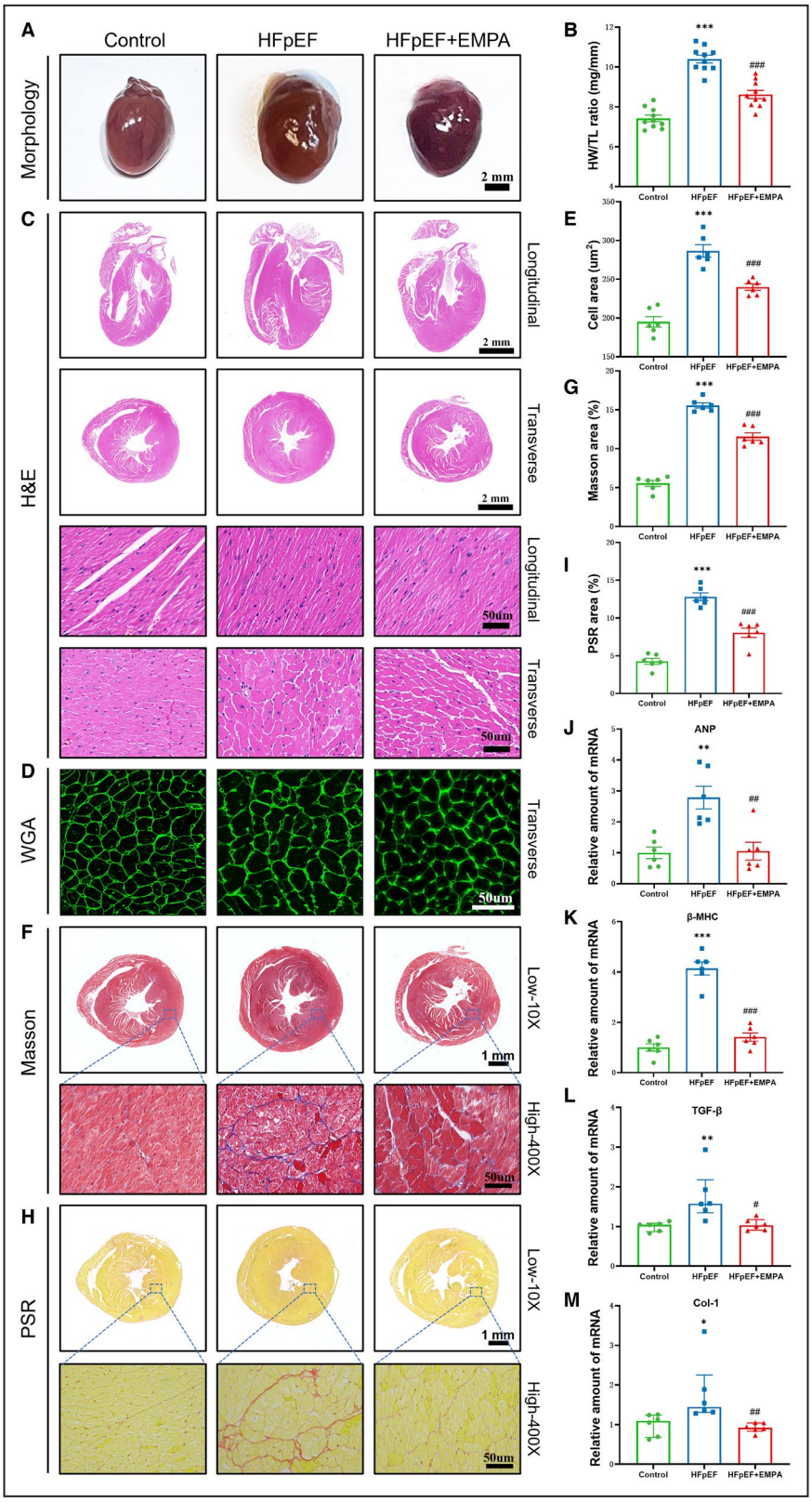

in a notable decrease in heart rate (Figure 1G). The outcomes of the intraperitoneal glucose tolerance tests indicated that glucose tolerance was significantly impaired in the HFpEF group compared with the control group but improved significantly following empagliflozin treatment (Figure 1H).

The serum levels of glucose, insulin, glycated albumin, Ang II, BNP (brain natriuretic peptide), and CRP (C-reactive

protein) were greater in the HFpEF group than in the control group but were lower after empagliflozin treatment (Table). Despite notable elevations in total cholesterol, triglyceride, low-density lipoprotein cholesterol, and high-density lipoprotein cholesterol levels in the HFpEF group, empagliflozin treatment did not significantly improve these lipid levels. Additionally, there were no significant differences in the creatinine or urea levels among the 3 groups.

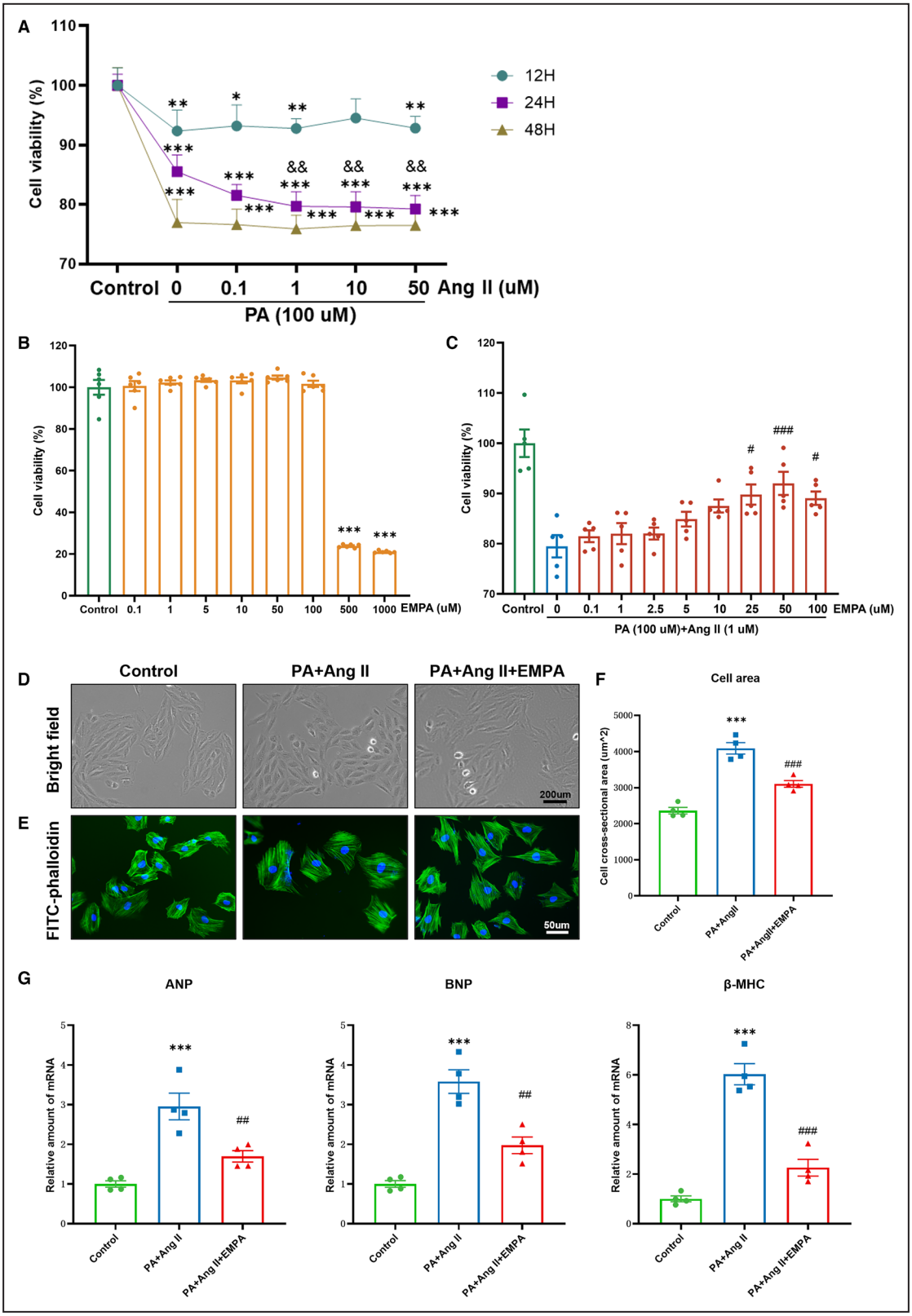

Figure 3. Empagliflozin reduces cardiomyocyte hypertrophy induced by Ang II and palmitate in vitro.
A, CCK-8 assay evaluating the viability of H9c2 cells treated with various concentrations of Ang II and palmitate over different time intervals (n=5). **B**, CCK-8 assay assessing the viability of H9c2 cardiomyocytes following treatment with different concentrations of EMPA (n=6). **C**, CCK-8 assay measuring the viability of H9c2 cells subjected to the "2-hit" model (100 μmol/L palmitate and 1 μmol/L Ang II for 24 hours) and then treated with varying concentrations of EMPA (n=5). **D**, Bright-field microscopy and (**E**) FITC–phalloidin staining images showing H9c2 cell morphology. **F**, Quantitative analysis of the H9c2 cell cross-sectional area in 4 independent experiments (n=4), with approximately 200 cells analyzed per group (μm^2). **G**, RT-qPCR analysis of the mRNA levels of the hypertrophic markers ANP, BNP, and β-MHC in H9c2 cells (n=4). The data are presented as mean±SEM. Statistical analyses were conducted using 2-way repeated measures ANOVA with Holm–Sidak post hoc tests (**A**) and 1-way ANOVA with Tukey's multiple comparison tests (**B**, **C**, **F**, **G**). Statistical significance: $^{*}P<0.05$, $^{**}P<0.01$, and $^{***}P<0.001$ vs the control; $^{\&\&}P<0.01$ vs the palmitate group; $^{\#}P<0.05$, $^{\#\#}P<0.01$, and $^{\#\#\#}P<0.001$ vs the "2-hit" model group. β-MHC indicates beta-myosin heavy chain; Ang II, angiotensin II; ANP, atrial natriuretic peptide; BNP, brain natriuretic peptide; CCK-8, Cell Counting Kit-8; EMPA, empagliflozin; PA, palmitate; and RT-qPCR, reverse transcription quantitative polymerase chain reaction.

As shown in the echocardiographic images (Figure 1I and 1J), there were no significant alterations in LVEF, LV fractional shortening, or LV internal dimension at end-diastole among the 3 groups of mice at the final cardiac function assessment (Figure 1K). Compared with those in untreated HFpEF mice, the increases in the LV mass, interventricular septum thickness at end-diastole, and LV posterior wall thickness at end-diastole in HFpEF mice treated with empagliflozin were significantly smaller (Figure 1L). Moreover, empagliflozin significantly improved diastolic function, as evidenced by favorable alterations in the E/A ratio, isovolumetric relaxation time, and deceleration time (Figure 1M).

Empagliflozin Attenuates Cardiac Hypertrophy and Fibrosis in HFpEF Mice

The gross morphology of the hearts (Figure 2A), heart weight to tibial length ratios (Figure 2B), and representative hematoxylin and eosin histological sections (Figure 2C) from the 3 experimental groups exhibited substantial cardiac hypertrophic changes in the HFpEF group, which were attenuated by empagliflozin treatment. To further evaluate cardiomyocyte hypertrophy, LV myocyte cross-sectional areas were measured via wheat germ agglutinin staining. As presented in Figure 2D and 2E, the cross-sectional areas of ventricular cardiomyocytes in HFpEF mice were significantly greater than those in control mice. Empagliflozin treatment dramatically alleviated the myocyte hypertrophy induced by high-fat diet plus L-NAME. Both Masson's staining (Figure 2F and 2G) and picrosirius red staining (Figure 2H and 2I) indicated increased interstitial and perivascular fibrosis in the HFpEF group compared with the control group, which was attenuated by empagliflozin treatment. At the molecular level, HFpEF-induced increases in hypertrophy-related markers, including ANP (atrial natriuretic peptide) and β-MHC (beta-myosin heavy chain), significantly decreased after empagliflozin administration (Figure 2J and 2K). Additionally, the mRNA expression levels of profibrotic markers, including TGF-β (transforming growth factor-beta) and Col-1 (collagen type I), were significantly increased in the HFpEF group, whereas empagliflozin significantly decreased these levels (Figure 2L and 2M). These results indicate that empagliflozin has profound cardioprotective effects on cardiac hypertrophy and fibrosis in HFpEF mice.

Empagliflozin Treatment Ameliorates Cardiomyocyte Hypertrophy in H9c2 Cells Induced by Palmitate and Ang II

To elucidate the role of empagliflozin in cardiomyocyte hypertrophy, an in vitro "2-hit" model of H9c2 cells was established in which palmitate combined with Ang II was used to mimic metabolic and pressure stress. A previous study showed that palmitate at a concentration of 75 μmol/L induced insulin resistance in H9c2 cells with minimal toxicity, resembling the diabetic state observed in humans and rats.[16] Furthermore, 100 μmol/L palmitate does not induce severe apoptosis in cardiomyocytes.[17] Consequently, our study employed a palmitate concentration of 100 μmol/L.

The results of the CCK-8 assay indicated that the viability of H9c2 cells significantly and persistently decreased at all tested concentrations of Ang II following 24 and 48 hours of exposure (Figure 3A). Compared with that of palmitate alone, cell viability was further reduced by the combined effect of Ang II and palmitate for 24 hours at concentrations of 1 μmol/L or higher (Figure 3A). On the basis of these findings, an in vitro "2-hit" model of cardiomyocyte hypertrophy was established by exposing H9c2 cells to a combination of palmitate and 1 μmol/L Ang II for 24 hours. The results of the CCK-8 assay also revealed that empagliflozin concentrations ranging from 0 to 100 μmol/L had no toxic or detrimental effects on normal H9c2 cells (Figure 3B). Notably, in the "2-hit" model, empagliflozin resulted in the most significant increase in cell viability at a concentration of 50 μmol/L (Figure 3C), which was employed for all subsequent experiments.

Under bright field microscopy, the "2-hit" stimulation group displayed the most pronounced increase in cell morphology among all groups (Figure 3D).

FITC–phalloidin staining further indicated a significant increase in the cross-sectional area of H9c2 cells in the "2-hit" model group, which was markedly reduced in cells treated with empagliflozin (Figure 3E and 3F). Additionally, compared with control conditions, concurrent stimulation with Ang II and palmitate

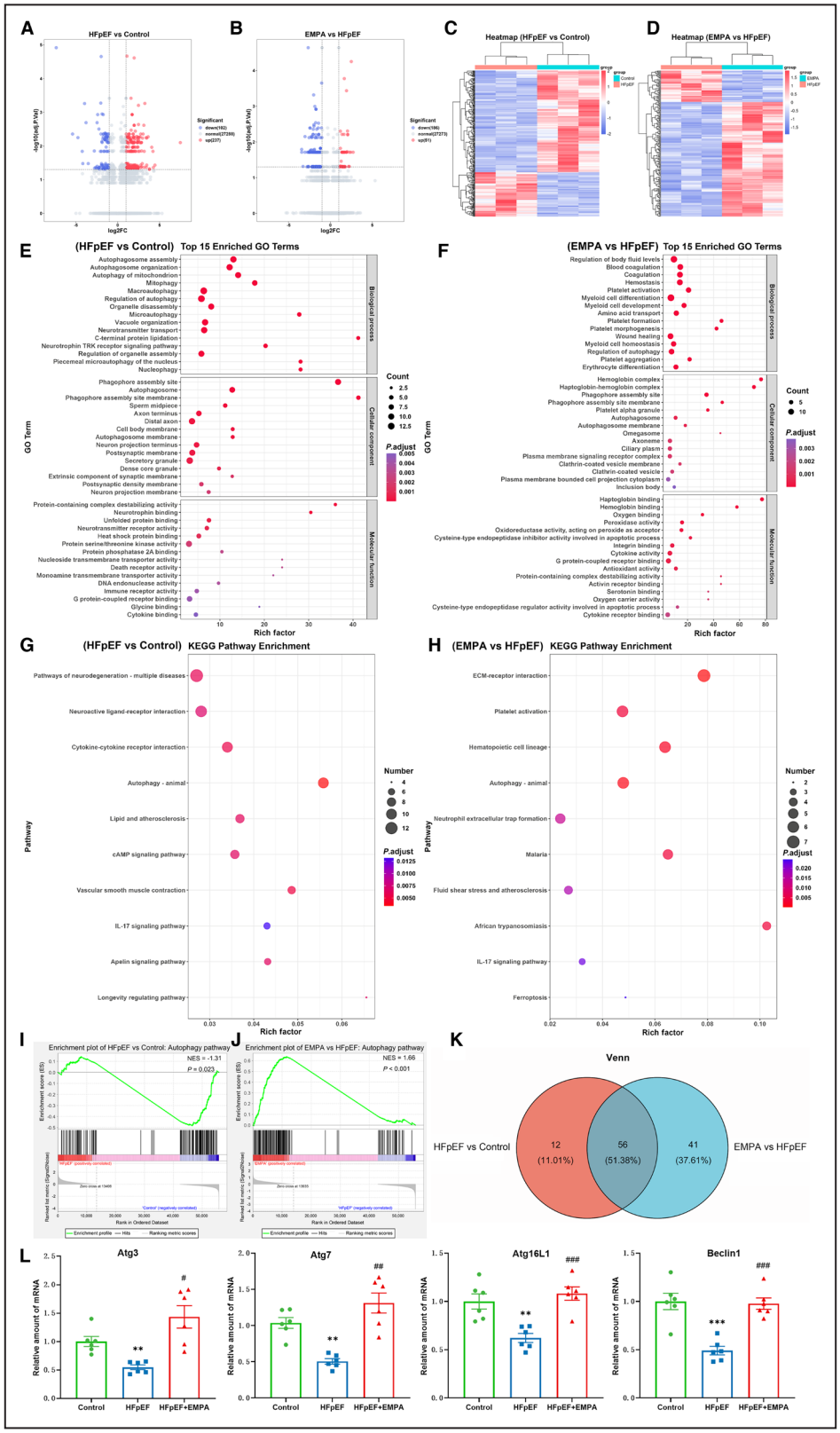

Figure 4. RNA sequencing and RT-qPCR analysis of autophagy-related genes in murine heart tissues.
A and **B**, Volcano plots showing DEGs in the HFpEF vs control groups (**A**) and EMPA-treated vs HFpEF groups (**B**). Dotted lines indicate statistical significance thresholds (|$\log_2$ fold change|>1 and false discovery rate-adjusted P<0.05; n=3 per group). **C** and **D**, Hierarchical clustering of DEGs in the HFpEF vs control (**C**) and EMPA vs HFpEF (**D**) groups. **E** and **F**, Top 15 GO terms enriched in DEGs from the HFpEF vs control (**E**) and EMPA vs HFpEF (**F**) comparisons. GO analysis revealed enrichment in processes such as neurotransmitter transport, autophagosome assembly, and cytokine secretion in the HFpEF vs control comparison; and platelet activation, autophagy formation, fluid regulation, and antioxidant activity in EMPA vs HFpEF. **G** and **H**, KEGG pathway enrichment of DEGs in the HFpEF vs control (**G**) and EMPA vs HFpEF (**H**). Significant pathways included neuroactive ligand-receptor interactions, autophagy, and cAMP signaling in HFpEF vs control; and extracellular matrix-receptor interaction, autophagy, and platelet activation in EMPA vs HFpEF. **I** and **J**, GSEA showing downregulation of autophagy-related gene expression in HFpEF vs control (NES=−1.31, P=0.023) and upregulation following EMPA treatment (NES=1.66, P<0.001). **K**, Venn diagram showing overlapping upregulated and downregulated DEGs across comparisons. **L**, RT-qPCR validation of selected autophagy-related DEGs (*Atg3*, *Atg7*, *Atg16L1*, *Beclin1*) in murine heart tissues (n=6 per group). Data are presented as mean±SEM. Statistical analyses were performed using 1-way ANOVA with Tukey's post hoc tests. $^{*}P$<0.05, $^{**}P$<0.01, $^{***}P$<0.001 vs control; $^{\#}P$<0.05, $^{\#\#}P$<0.01, $^{\#\#\#}P$<0.001 vs HFpEF. DEGs indicates differentially expressed genes; EMPA, empagliflozin; GO, Gene Ontology; GSEA, gene set enrichment analysis; HFpEF, heart failure with preserved ejection fraction; IL-17, interleukin 17; KEGG, Kyoto Encyclopedia of Genes and Genomes; NES, normalized enrichment score; and RT-qPCR, reverse transcription quantitative polymerase chain reaction.

significantly increased the mRNA levels of ANP, BNP, and β-MHC, whereas empagliflozin treatment significantly attenuated these levels (Figure 3G).

These results support our in vivo findings, suggesting that empagliflozin treatment can potentially mitigate "2-hit"-induced cardiac hypertrophy.

Empagliflozin Exerts Cardioprotective Effects Via Autophagy-Associated Signaling Based on RNA-Seq Analysis

To further explore the molecular mechanisms underlying the cardioprotective effects of empagliflozin in HFpEF, RNA sequencing of LV tissues was performed. The volcano plot displayed 237 upregulated and 102 downregulated genes in the HFpEF group compared with the control group (Figure 4A). In the HFpEF+empagliflozin group, 51 genes were upregulated, whereas 186 genes were downregulated compared with those in the HFpEF group (Figure 4B). The cluster heatmap demonstrated consistent expression patterns of DEGs within each group (Figure 4C and 4D). Gene Ontology enrichment analysis revealed that the DEGs in the HFpEF group were predominantly associated with autophagy, synaptic signaling, and cytokine secretion (Figure 4E). In contrast, the empagliflozin-treated group presented significant changes in the expression of genes related to fluid regulation, blood coagulation, and cellular autophagy (Figure 4F). Kyoto Encyclopedia of Genes and Genomes enrichment analysis showed that the DEGs in the HFpEF group were enriched in pathways such as neuroactive ligand-receptor interactions, autophagy, and cAMP signaling pathway (Figure 4G). empagliflozin treatment induced significant alterations in the expression of genes involved in autophagy, extracellular matrix-receptor interaction, and platelet activation pathways (Figure 4H). More important, both Gene Ontology and Kyoto Encyclopedia of Genes and Genomes analyses highlight the significant role of autophagy in empagliflozin-mediated cardioprotection against HFpEF, suggesting that autophagy may be a key mechanism in this process. Building on the SGLT2i-autophagy hypothesis proposed in previous literature,[18,19] we further conducted gene set enrichment analysis of the autophagy pathway. Gene set enrichment analysis showed that 68 autophagy-related genes were downregulated in the HFpEF group, whereas 97 genes were significantly upregulated after empagliflozin treatment (Figure 4I and 4J). Venn analysis revealed 56 autophagy-related genes common to both groups, including *Atg3*, *Atg7*, *Atg16L1*, and *Beclin1* (Figure 4K). To further verify the involvement of autophagy-associated signaling in empagliflozin-modulated cardioprotection against HFpEF, reverse transcription quantitative polymerase chain reaction experiments were performed. The results revealed a significant downregulation of autophagy-related markers following high-fat diet and L-NAME administration, whereas empagliflozin treatment reversed this trend and induced the upregulation of these markers (Figure 4L). On the basis of the aforementioned findings from the RNA-seq analysis, we supported that autophagy signaling may mediate the cardioprotective effects of empagliflozin in HFpEF.

Empagliflozin Regulates AMPK/mTOR Complex 1/Autophagy Signaling to Inhibit HFpEF In Vivo

To further investigate the effect of empagliflozin on autophagy in the "2-hit" mouse model of HFpEF, we first examined autophagy-related morphological and structural changes in cardiomyocytes via transmission electron microscopy. The resulting images revealed autophagosomes and autolysosomes in the control group (Figure 5A). In contrast, the HFpEF group presented disordered myocardial filaments, increased fat droplets and glycogen particles, and impaired mitochondrial integrity without the presence of autophagosomes (Figure 5A). Empagliflozin treatment improved

the mitochondrial structure and reduced glycogen granule deposition and fat droplet distribution, with an increased presence of lysosomes and autolysosomes undergoing degradation. Furthermore, the levels of autophagy-related proteins in the myocardium were further assessed by Western blot, immunohistochemistry, and immunofluorescence analyses. The Western blot results showed the decreased expression levels

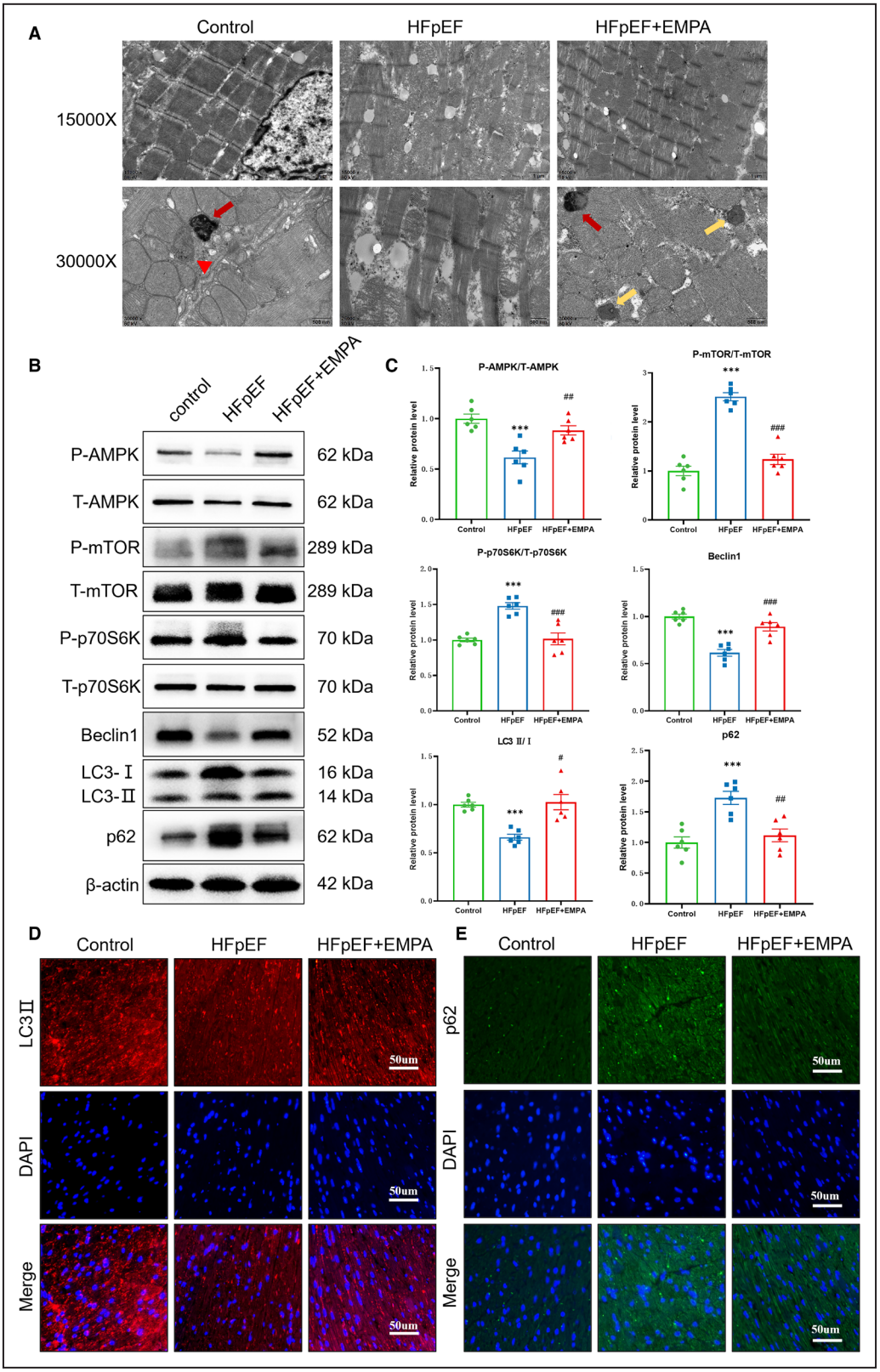

Figure 5. Empagliflozin regulates AMPK/mTORC1/autophagy signaling in HFpEF mice.
A, Transmission electron microscopy images of the left ventricular myocardium from the control, HFpEF, and HFpEF+EMPA groups. In the control group, the myocardial filaments were well organized, with intact mitochondrial morphology and regular double-membrane structures. Autophagosome (red triangle) and autolysosome (red arrow) were observed. In the HFpEF group, the myocardial filaments were disordered, with some broken, dissolved, or absent mitochondrial cristae, and the electron density decreased. Fat droplets and glycogen particles were prevalent, with no autophagosomes or autolysosomes visible. In the HFpEF+EMPA group, the myocardial filaments were relatively well organized, the mitochondrial crista structure was improved, and the electron density was restored. More lysosomes (yellow arrows) and autolysosomes (red arrows) were visible. **B**, Western blot bands and (**C**) statistical analyses of the effects of EMPA on the AMPK/mTORC1/autophagy pathway. The data were normalized to total protein (for phosphorylated protein) and β-Actin (for total protein) and are expressed as the fold change relative to the control (n=6). **D**, LC3-II immunofluorescence staining in murine left ventricular tissue. **E**, p62 immunofluorescence staining in murine left ventricular tissue. Fluorescent puncta represent antibody-specific target protein, images were captured at 400× magnification (scale bar: 50 μm). The data are presented as mean±SEM (n=6 per group). Statistical tests were conducted using 1-way ANOVA with Tukey's multiple comparisons. Statistical significance: $^{*}P<0.05$, $^{**}P<0.01$, and $^{***}P<0.001$ vs the control group; $^{\#}P<0.05$, $^{\#\#}P<0.01$, and $^{\#\#\#}P<0.001$ vs the HFpEF group. AMPK indicates AMP-activated protein kinase; EMPA, empagliflozin; HFpEF, heart failure with preserved ejection fraction; LC3-II, microtubule-associated protein 1 light chain 3; mTORC1, mammalian target of rapamycin complex 1; P-AMPK, phosphorylated AMPK; P-mTOR, phosphorylated mammalian target of rapamycin; and P-p70S6K, phosphorylated p70S6K.

of the autophagy markers LC3-II and Beclin1 but increased expression of the autophagy substrate p62 in the "2-hit" model mice compared with the controls (Figure 5B and 5C). Notably, empagliflozin administration significantly elevated LC3-II expression and decreased p62 levels, indicating increased autophagy. These findings were further corroborated by immunofluorescence staining for LC3-II (Figure 5D) and p62 (Figure 5E), as well as immunohistochemical staining for Beclin1 (Figure 6A).To elucidate the specific mechanisms involved in cardiomyocyte autophagy, we analyzed the classical upstream regulators of autophagy, including AMPK and mTOR, via Western blotting in conjunction with transcriptomics data. Our results revealed a reduced phospho-AMPK (P-AMPK)/total AMPK (T-AMPK) ratio in HFpEF mice, which was significantly increased in empagliflozin-treated mice (Figure 5B and 5C). Additionally, the HFpEF group presented increased phosphorylation of mTOR complexes and their downstream mediators, p70-S6K, relative to the control group. These alterations were completely reversed by empagliflozin treatment (Figure 5B and 5C). The immunohistochemistry results for P-AMPK and phospho-mTOR (P-mTOR) further corroborated the Western blot findings (Figure 6B through 6D). Collectively, these comprehensive outcomes indicate that the AMPK–mTORC1 (mTOR complex 1) pathway may be responsible for the enhanced cardiomyocyte autophagy in empagliflozin-mediated defense against HFpEF.

Empagliflozin Alleviates Cardiac Hypertrophy Through the Regulation of AMPK/mTORC1/Autophagy Signaling In Vitro

We also investigated the potential mechanisms in cultured H9c2 cells. First, we used Western blotting to evaluate the effects of empagliflozin on Beclin1, LC3-II, and p62 expression in Ang II- and palmitate-stimulated H9c2 cells. The results showed that "2-hit" stimulation reduced LC3-II and Beclin1 levels but increased p62 expression (Figure 7A and 7B). In contrast, empagliflozin treatment significantly increased LC3-II and Beclin1 expression while inhibiting p62 expression, indicating that autophagy was restored by empagliflozin treatment in cultured H9c2 cells (Figure 7A and 7B). In vivo studies have demonstrated that AMPK negatively regulates mTOR to trigger autophagy. The phosphorylation levels of AMPK and mTOR were subsequently analyzed in vitro (Figure 7A and 7B). Palmitate and Ang II were found to inhibit AMPK phosphorylation and promote mTOR phosphorylation, resulting in impaired autophagic initiation. However, empagliflozin treatment resulted in increased P-AMPK expression and decreased P-mTOR and P-p70S6K levels compared with those in the "2-hit" cells.

To elucidate the role of AMPK in mediating the protective effect of empagliflozin on "2-hit"-induced HFpEF. Compound C (CC, 5 μmol/L), a specific AMPK inhibitor, was used in our study. The Western blot results revealed that CC inhibited AMPK phosphorylation, activated mTOR and p70S6K phosphorylation, and suppressed autophagy in the empagliflozin-treated group (Figure 7C and 7D). These findings suggest that activated AMPK negatively regulates mTORC1, thereby enhancing the autophagy pathway, which contributes to empagliflozin-induced protective effects in H9c2 cells.

To comprehensively investigate empagliflozin-mediated modulation of autophagic flux through the AMPK/mTORC1 pathway, we performed mRFP-GFP-LC3 autophagic flux assays and included 2 additional intervention groups: one treated with the AMPK inhibitor CC (5 μmol/L) and the other with the autophagy inhibitor MHY1485 (5 μmol/L). As shown in Figure 7B and 8B, autophagic flux analysis showed that the "2-hit" stimulation with palmitate and Ang II significantly reduced the numbers of autophagosomes and autolysosomes in H9c2 cardiomyocytes. In contrast, empagliflozin treatment markedly increased both autophagosome and

autolysosome accumulation compared with the model group, indicating enhanced autophagic flux. Notably, this empagliflozin-induced activation of autophagy was substantially attenuated in the presence of CC or MHY1485, with both inhibitor groups showing significantly lower autophagic flux compared with the empagliflozin-treated group. These findings demonstrate that empagliflozin promotes the full autophagic flux—from early

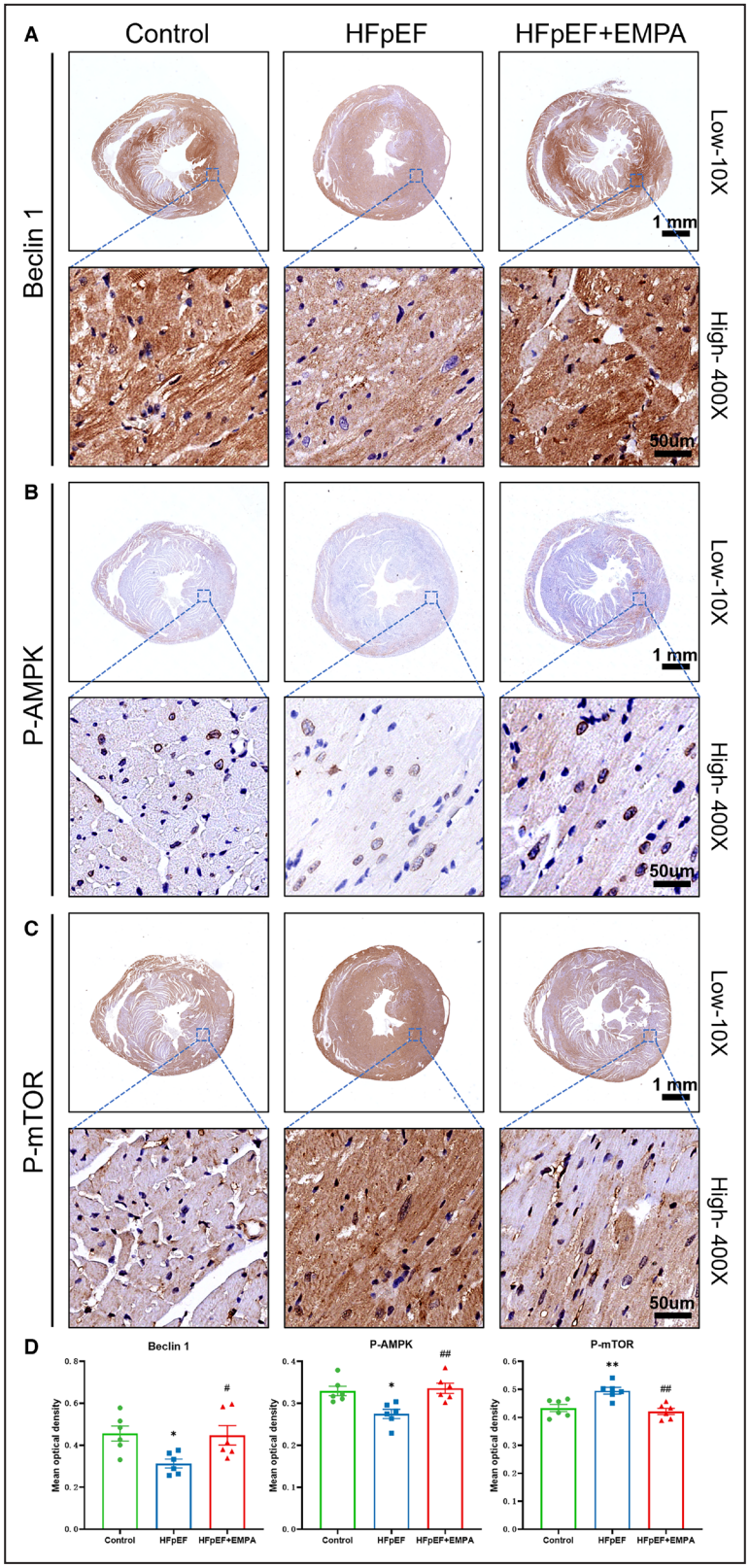

Figure 6. Empagliflozin regulates Beclin1, P-AMPK, and P-mTOR levels in HFpEF mice.
A through **C**, Representative immunohistochemical staining images and (**D**) quantitative analyses of Beclin1, P-AMPK, and P-mTOR in the murine left ventricular tissue. EMPA significantly elevated Beclin1 and P-AMPK expression, while decreased P-mTOR levels compared with the HFpEF group. The data are presented as mean±SEM (n=6 per group). Statistical tests were conducted using 1-way ANOVA with Tukey's multiple comparisons. Statistical significance: $^{*}P<0.05$, $^{**}P<0.01$, and $^{***}P<0.001$ vs the control group; $^{\#}P<0.05$, $^{\#\#}P<0.01$, and $^{\#\#\#}P<0.001$ vs the HFpEF group. EMPA indicates empagliflozin; HFpEF, heart failure with preserved ejection fraction; P-AMPK, phosphorylated AMP-activated protein kinase; and P-mTOR, phosphorylated mammalian target of rapamycin.

autophagosome formation to late autophagolysosomal degradation—via AMPK/mTORC1 signaling.

Lastly, to further establish the functional linkage between the AMPK/mTORC1/autophagy pathway and empagliflozin-induced antihypertrophic effects, we quantified cardiomyocyte size via FITC-phalloidin staining across 5 experimental groups. As shown in Figure 8C, significant enlargement of the cell areas was observed in the CC and MHY1485 groups compared with the empagliflozin-treated group. The finding confirmed that both the AMPK inhibitor CC and the autophagy inhibitor MHY1485 nullified the protective effect of empagliflozin on cardiomyocyte hypertrophy through this pathway.

In summary, these findings demonstrated that empagliflozin ameliorated cardiomyocyte hypertrophy by regulating the AMPK/mTORC1/autophagy pathway.

DISCUSSION

To our knowledge, this study is the first to elucidate the beneficial effects of empagliflozin in the "2-hit" mouse model of HFpEF induced by a combination of high-fat diet and L-NAME via an autophagy-dependent mechanism. The major findings of this research are as follows: (1) empagliflozin attenuates HFpEF-induced diastolic dysfunction and ventricular remodeling, characterized by reduced left ventricular hypertrophy and cardiac fibrosis; (2) empagliflozin effectively inhibits cardiomyocyte hypertrophy in vitro; (3) RNA-seq analysis reveals that autophagy signaling is a critical mediator of the cardioprotective effect of empagliflozin in HFpEF; and (4) the amelioration of cardiomyocyte hypertrophy by empagliflozin is mediated by the AMPK/mTORC1/autophagy signaling pathway.

Effects of Empagliflozin on Cardiac Remodeling in HFpEF

The osmotic diuresis and natriuresis effects of SGLT2i on the renal proximal tubule lead to a modestly reduced circulation volume and improved BP control, benefiting patients with HF.[20] However, these properties may not elucidate the primary mechanisms of SGLT2i in HFpEF.[21,22] Furthermore, stronger diuretics, such as loop diuretics, do not significantly reduce adverse events in patients with HFpEF. Consequently, the direct metabolic effects of SGLT2i on HFpEF have become a focal point of investigation.

In this study, the "2-hit" model of cardiometabolic HFpEF mice primarily exhibited metabolic disorders, including obesity, hypertension, and glucose intolerance, leading to subsequent cardiac remodeling characterized by cardiomyocyte hypertrophy and cardiac fibrosis. Moreover, empagliflozin significantly attenuated LV remodeling and diastolic dysfunction in HFpEF, as evidenced by alterations in the cardiomyocyte cross-sectional area, extent of fibrosis, and echocardiographic parameters of diastolic function. The reduction in cardiac hypertrophy and LV mass has been recognized as a crucial determinant of improved outcomes in HF condition.[23,24] Recent clinical trials have shown the effects of SGLT2i on LV remodeling in patients with type 2 diabetes, coronary artery disease, and prevalent HF with reduced EF.[25,26] However, research on the effects of SGLT2i on cardiac remodeling in HFpEF is limited, and the available data remain sparse. In a nondiabetic rodent model of HFpEF, empagliflozin improved diastolic function and reduced wall stress by ameliorating myocyte hypertrophy without fibrotic collagen I/IV.[27] Our findings support the hypothesis that empagliflozin attenuates adverse cardiac remodeling, characterized by cardiomyocyte hypertrophy and cardiac fibrosis, through the modulation of the TGF-β/collagen I pathway.

Empagliflozin decreased the expression of the hypertrophic markers ANP, BNP, and β-MHC, which was accompanied by improvements in glucose metabolism and insulin resistance in HFpEF mice. However, empagliflozin did not induce significant alterations in lipid parameters, which is consistent with previous findings of its modest influence on plasma lipid profiles.[20,28] Furthermore, alterations in serum CRP and Ang II levels suggest that empagliflozin attenuates excessive inflammatory responses and overactivation of the renin–angiotensin–aldosterone system, providing meaningful insights for identifying biochemical markers with predictive value for HFpEF treatment.

Involvement of Autophagy in Empagliflozin-Modulated Defense Against HFpEF

To elucidate the molecular mechanisms underlying the cardioprotective effects of empagliflozin in attenuating

cardiac remodeling, transcriptomics LV tissues was performed. Our findings suggest that autophagy signaling is involved in both the pathogenesis of HFpEF and the therapeutic effects of empagliflozin. Specifically, the expression of autophagy-related genes was lower in the HFpEF group than in the control group, whereas empagliflozin treatment resulted in their upregulation. Transcriptomic analysis in humans with HFpEF or HF with reduced EF

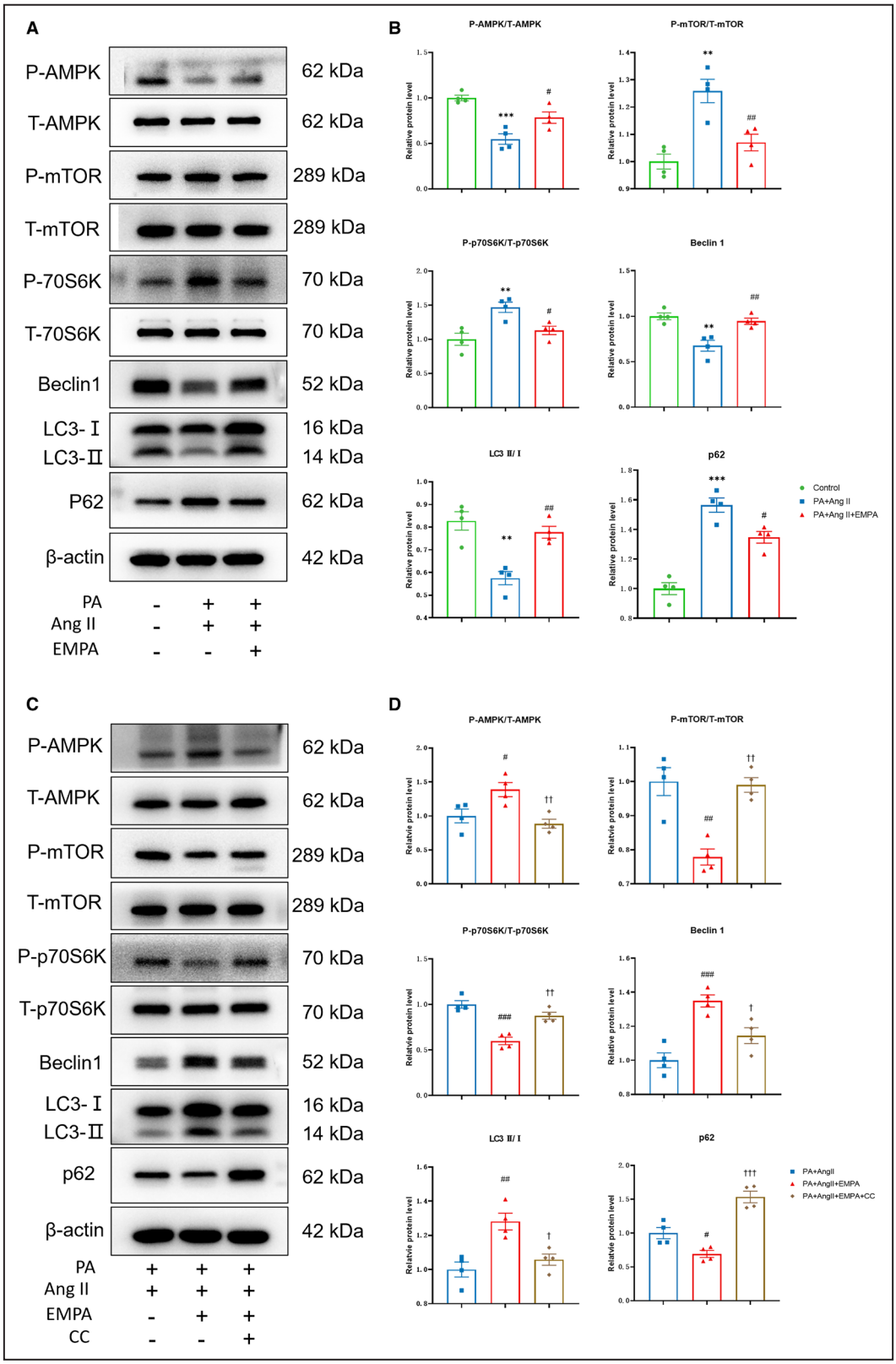

Figure 7. Empagliflozin modulates the AMPK/mTORC1/autophagy pathway in vitro.
A, Western blot bands and (**B**) statistical analysis showing the effects of EMPA on the AMPK/mTORC1/autophagy pathway in the "2-hit" H9c2 cell model. The "2-hit" model decreased the expression of P-AMPK, LC3-II, and Beclin1 while increasing P-mTOR, P-p70S6K, and p62 levels. EMPA treatment significantly increased P-AMPK, LC3-II, and Beclin1 levels but inhibited P-mTOR, P-p70S6K, and p62 levels (n=4). The data were normalized to total protein (for phosphorylated proteins) and β-actin (for total protein) and are expressed as the fold change relative to the control group. **C**, Western blot bands and (**D**) statistical analysis showing the effect of CC (5 μmol/L) on the AMPK/mTORC1/autophagy pathway in H9c2 cells treated with EMPA (50 μmol/L). Compared with EMPA, CC significantly decreased the levels of P-AMPK, LC3-II, and Beclin1 but increased the P-mTOR, P-p70S6K, and p62 levels. The data were normalized to total protein (for phosphorylated protein) and β-actin (for total protein) and expressed as the fold change relative to the palmitate+Ang II group (n=4). Statistical analyses were conducted using 1-way ANOVA with Tukey's multiple comparison tests. Statistical significance: $^{*}P<0.05$, $^{**}P<0.01$, $^{***}P<0.001$ vs the control group; $^{\#}P<0.05$, $^{\#\#}P<0.01$, $^{\#\#\#}P<0.001$ vs the palmitate+Ang II group. AMPK indicates AMP-activated protein kinase; Ang II, angiotensin II; CC, compound C; EMPA, empagliflozin; LC3-II, microtubule-associated protein 1 light chain 3; mTORC1, mammalian target of rapamycin complex 1; PA, palmitate; P-AMPK, phosphorylated AMP-activated protein kinase; P-mTOR, phosphorylated mammalian target of rapamycin; and P-p70S6K, phosphorylated p70S6K.

revealed that the genes associated with autophagy and endoplasmic reticulum stress were specifically downregulated in HFpEF.[29] Recent proteomics analysis of pooled data from 535 patients in the EMPEROR-Preserved trial demonstrated significant effects of empagliflozin on proteins involved in cardiac autophagy and hypertrophy.[30] These findings collectively support the hypothesis that cellular autophagy mediates the therapeutic benefits of SGLT2i in patients with HFpEF.

Autophagy, a highly conserved process for degrading damaged cytoplasmic contents, plays a critical role in the pathogenesis of cardiac hypertrophy and is often triggered by various stimuli. A high-fat diet induces cardiac hypertrophy while concurrently suppressing autophagy through the inhibition of AMPK phosphorylation and subsequent activation of mTOR phosphorylation in the heart. Conversely, mechanical stretch or Ang II insult elicits enhanced cardiomyocyte autophagy, contributing to cardiomyocyte hypertrophy.[31] The present study demonstrated that a "2-hit" model of failing myocardium combining a high-fat diet with pressure overload is associated with hypertrophic remodeling and concurrent autophagy insufficiency, as evidenced by RNA sequencing and quantitative analysis of autophagy-related proteins. Notably, empagliflozin attenuated cardiac hypertrophy through enhancing autophagy, which aligns with previous findings supporting the cardioprotective role of autophagy.[32] It has been reported that, similar to obesity, HF is characterized by the intracellular accumulation of glucose and lipid intermediates, which are perceived by cells as indicators of energy overabundance, thus leading to an impairment of autophagic flux and acceleration of cardiomyopathy.[18,33] Moreover, the administration of SGLT2i could reverse this maladaptive signaling, thereby promoting cardiac homeostasis and adaptive responses to stress.[19]

Beyond its beneficial effects on cardiac remodeling in HFpEF, SGLT2i has demonstrated therapeutic efficacy in conditions such as obesity, diabetes, and myocardial damage through cellular autophagy. For example, dapagliflozin activated autophagy to protect against high glucose-induced endothelial cell injury[34] and reduced pancreatic oxidative stress and inflammation in obese rats.[35] In addition, empagliflozin stimulated glomerular autophagy and exerted renoprotective effects in type 2 diabetes.[36] Interestingly, in diabetic cardiomyopathy, empagliflozin improved cardiac fibrosis and heart function through either inhibiting excessive autophagy in diabetic mice receiving a single intraperitoneal injection of streptozotocin[37] or enhancing autophagy in diabetic KK Cg-Ay/J mice.[38] This discrepancy in autophagy between these studies might be attributed to the use of distinct diabetes models and varying disease progression stages. These findings also indicate that cellular autophagy is a critical mechanism involved in the therapeutic effects of SGLT2i across various tissues and cells. Our study demonstrates the important role of autophagy in the "2-hit" murine model of HFpEF, which deepens the understanding of autophagy dysregulation in cardiovascular disorders and suggests the potential for targeting metabolic disturbances through pharmacological modulation of autophagy.

Empagliflozin Regulates Autophagy Via the AMPK/mTORC1 Pathway

Among the molecular mediators involved in SGLT2i-induced cardiomyocyte autophagy, the nutrient-deprivation sensors AMPK and mTOR are particularly important. AMPK, a serine/threonine protein kinase, negatively regulates mTOR and positively activates autophagy initiation molecules. Conversely, the level of mTORC1, a multiprotein complex of mTOR, is reduced in nutrient-deprived cells, leading to autophagy activation and decreased protein synthesis via phosphorylation of the downstream target p70S6K. In the context of HF, the regulation of these mediators, which are essential for maintaining energy and metabolic homeostasis, is often disrupted, and AMPK activity is typically inhibited in the failing myocardium.[39]

It is postulated that SGLT2i may induce a state of fasting mimicry, thereby increasing the activities of

AMPK and other low-energy sensors, which activate downstream signaling in HFpEF.[39] Our mechanistic study demonstrated that empagliflozin treatment in HFpEF mice resulted in AMPK activation and mTORC1 inhibition, which augmented autophagy and alleviated cardiomyocyte hypertrophy. These findings suggest that empagliflozin effectively rebalances metabolic disturbances and promotes cardiomyocyte autophagy

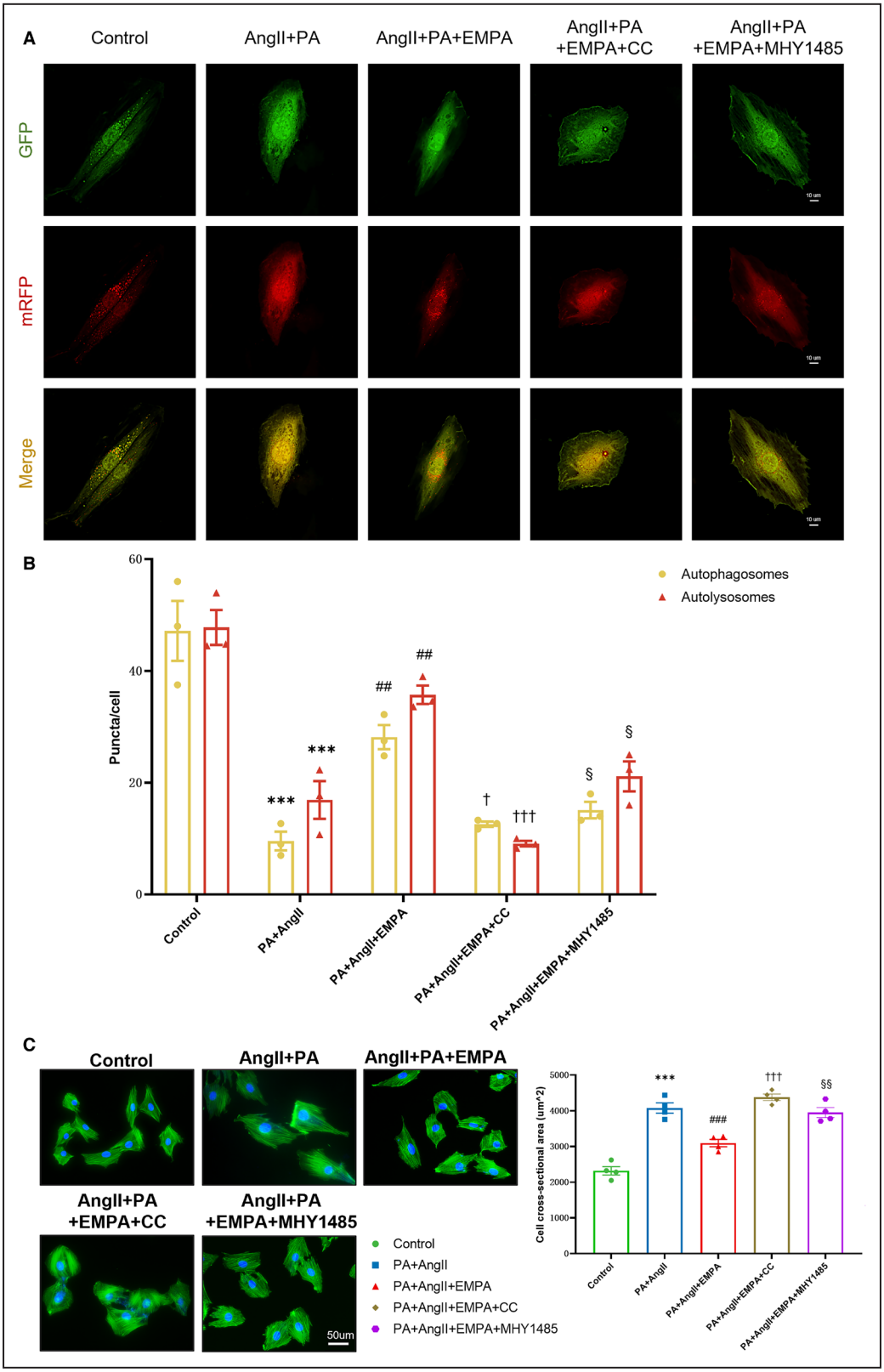

Figure 8. Empagliflozin modulates AMPK/mTORC1/autophagy signaling to mitigate cardiomyocyte hypertrophy.
A, Confocal images of mRFP-GFP-LC3 puncta in H9c2 cells under indicated treatments (scale bar: 10 μm). Representative autophagosomes (yellow puncta) and autolysosomes (red puncta) are shown. **B**, Quantification of puncta demonstrates that Compound C (AMPK inhibitor) and MHY1485 (autophagy inhibitor) antagonize EMPA-induced increases in autophagosomes and autolysosomes. Data are mean±SEM from 3 independent experiments (9–14 cells/group). **C**, FITC–phalloidin staining of H9c2 cells, illustrating cell hypertrophy. The effects of the AMPK inhibitor CC (5 μmol/L) and the autophagy inhibitor MHY 1485 (5 μmol/L) on cell morphology are shown. The cell areas (μm^2) were quantified in 4 independent experiments, with approximately 200 cells counted per group. The data are presented as mean±SEM. Statistical tests were conducted using 1-way ANOVA with Tukey's multiple comparisons. Statistical significance: $^{*}P<0.05$, $^{**}P<0.01$, $^{***}P<0.001$ vs the control group; $^{\#}P<0.05$, $^{\#\#}P<0.01$, $^{\#\#\#}P<0.001$ vs the palmitate+Ang II group; $^{\dagger}P<0.05$, $^{\dagger\dagger}P<0.01$, $^{\dagger\dagger\dagger}P<0.001$ vs the palmitate+Ang II+EMPA group; $^{\S}P<0.05$, $^{\S\S}P<0.01$ vs the palmitate+Ang II+EMPA group. Ang II indicates angiotensin II; CC, compound C; EMPA, empagliflozin; GFP, green fluorescent protein; LC3, microtubule-associated protein 1 light chain 3; mRFP, monomeric red fluorescent protein; mTORC1, mammalian target of rapamycin complex 1; and PA, palmitate.

via the AMPK/mTORC1 axis, contributing to improved structural remodeling. This evidence underscores empagliflozin's role as a direct cardioprotective agent and highlights the AMPK/mTORC1/autophagy pathway as a critical target in managing cardiometabolic HFpEF.

The AMPK/mTOR-mediated autophagy pathway also plays a pivotal role in the therapeutic effects of SGLT2i on other stress conditions. For instance, dapagliflozin restored autophagy via the AMPK/mTOR pathway to mitigate advanced glycation end product-induced podocyte injury[40] and hepatic lipid accumulation.[41] Similarly, empagliflozin reduced neurobehavioral deficits[42] and sunitinib-induced cardiac dysfunction[43] by enhancing autophagy via the AMPK/mTOR pathway. Additionally, by activating AMPK, empagliflozin protected the heart from inflammation and energy depletion, demonstrating the multiple protective effects of SGLT2i-activated AMPK in various pathological conditions.[44]

Study Limitations

First, we selected C57BL/6N mice as the experimental model for the cardiometabolic HFpEF study based on previous research. However, male C57BL/6N mice are more prone to developing HFpEF features compared with females, which contrasts with the higher prevalence of HFpEF in women observed in human populations. Recent study has demonstrated that both male and female C57BL/6J mice can develop "2-hit" HFpEF, with female mice exhibiting more pronounced HFpEF phenotypes.[45] Given the differences in genetic backgrounds among mouse strains, C57BL/6J mice may represent a more suitable animal model for mimicking the human HFpEF pathogenesis. Furthermore, HFpEF is a heterogeneous clinical syndrome, and our study used a specific "2-hit" model focusing on hypertension and obesity to induce cardiometabolic HFpEF. Namely, our research did not investigate the mechanisms underlying HFpEF caused by other comorbidities, such as aging, chronic kidney dysfunction, atrial fibrillation and chronic obstructive pulmonary disease. Therefore, our findings should be extrapolated to other HFpEF phenogroups with caution. Second, our cardiac functional assessment did not include LV pressure-volume measurements, which are more direct and sensitive for evaluating diastolic dysfunction. However, noninvasive echocardiography allows for repeated assessments and avoids surgical interference with growth and feeding in obese mice, contributing to a more stable HFpEF model. Therefore, a majority of studies involving obese mice prefer noninvasive echocardiography for cardiac function monitoring and pressure-volume loop examination could be implemented at the end of animal experiments. Third, although we identified the AMPK/mTORC1/autophagy pathway through transcriptomic analysis and confirmed the antihypertrophic effects of empagliflozin in cell experiments, further validation of the effects of various autophagy inhibitors in HFpEF animal tissues is required to comprehensively assess the protective mechanisms of SGLT2i via autophagy. Addressing this gap will constitute our primary research focus moving forward. Fourth, our study focused on the role of AMPK in mediating autophagy in the therapeutic effects of empagliflozin against HFpEF. However, the specific mechanisms underlying the activation of AMPK remain unclear. Emerging evidence suggests that SGLT2i may regulate downstream proteinase activity by inhibiting the cell membrane receptor Na/H exchanger-1 or activating AMPK through "nutrient deprivation" effects involving sirtuins, particularly SIRT1 and SIRT3.[5,46] Investigating the mechanisms by which AMPK activity is elevated in the SGLT2i-treated HFpEF milieu represents a valuable area for future research. Lastly, this study primarily explored the direct effects of SGLT2 inhibition on myocardial remodeling in HFpEF. However, noncardiomyocyte populations, including fibroblasts and endothelial cells, may contribute to fibrosis progression, vascular dysfunction, and inflammation in HFpEF. Future research should investigate the mechanisms of SGLT2 inhibitors on profibrotic remodeling in these cell types.

CONCLUSIONS

In conclusion, empagliflozin treatment ameliorates LV remodeling with a concomitant improvement in

diastolic dysfunction in "2-hit" HFpEF mice, and this protective effect is mediated by the inhibition of cardiac hypertrophy through the restoration of AMPK/mTORC1-induced autophagy. These findings provide new and supportive insights into the clinical applications of SGLT2i in the treatment of HFpEF. Further research targeting the autophagy process and its associated mediators, as suggested by this study, holds promise for the development of novel therapeutic strategies in patients with HFpEF.

ARTICLE INFORMATION

Received December 10, 2024; accepted June 26, 2025.

Affiliations

Department of Cardiovascular Medicine, The Second Affiliated Hospital of Chongqing Medical University, Chongqing, China (X.H., D.L., W.C., H.K., D.Y., Y.L., G.L., K.W., M.X., Y.X., Y.Y.); Chongqing Key Laboratory of Arrhythmias, Chongqing, China (X.H., D.L., W.C., H.K., D.Y., Y.L., G.L., K.W., M.X., Y.X., Y.Y.); Chongqing Cardiac Arrhythmias Therapeutic Service Center, Chongqing, China (W.C., D.Y., Y.X., Y.Y.); Department of Cardiology, Chongqing University Fuling Hospital, Chongqing, China (X.H.); and Department of Ultrasound Medicine, The First Affiliated Hospital of Chongqing Medical University, Chongqing, China (Z.G.).

Acknowledgments

We thank Mr Lingkun Song for assisting with the graphical abstract and all those who helped during this experimental research. Additionally, we are deeply appreciative of the reviewers for their valuable and kind comments.

Sources of Funding

This work was supported by the Natural Science Foundation of Chongqing Municipality (Postdoctoral Funding: CSTB2022NSCQ-BHX0642) and the National Natural Science Foundation of China (Grant No. 32071110).

Disclosures

None.

Supplemental Material

Data S1
Table S1

REFERENCES

1. Savarese G, Becher PM, Lund LH, Seferovic P, Rosano G, Coats A. Global burden of heart failure: a comprehensive and updated review of epidemiology. *Cardiovasc Res*. 2023;118:3272–3287. doi: 10.1093/cvr/cvac013
2. McDonagh TA, Metra M, Adamo M, Gardner RS, Baumbach A, Bohm M, Burri H, Butler J, Celutkiene J, Chioncel O, et al. 2021 ESC guidelines for the diagnosis and treatment of acute and chronic heart failure. *Eur Heart J*. 2021;42:3599–3726. doi: 10.1093/eurheartj/ehab368
3. Anker SD, Butler J, Filippatos G, Ferreira JP, Bocchi E, Bohm M, Brunner-La RH, Choi DJ, Chopra V, Chuquiure-Valenzuela E, et al. Empagliflozin in heart failure with a preserved ejection fraction. *N Engl J Med*. 2021;385:1451–1461. doi: 10.1056/NEJMoa2107038
4. Vallon V, Verma S. Effects of SGLT2 inhibitors on kidney and cardiovascular function. *Annu Rev Physiol*. 2021;83:503–528. doi: 10.1146/annurev-physiol-031620-095920
5. Chen S, Wang Q, Bakker D, Hu X, Zhang L, van der Made I, Tebbens AM, Kovacshazi C, Giricz Z, Brenner GB, et al. Empagliflozin prevents heart failure through inhibition of the NHE1-NO pathway, independent of SGLT2. *Basic Res Cardiol*. 2024;119:751–772. doi: 10.1007/s00395-024-01067-9
6. Wu Q, Yao Q, Hu T, Yu J, Jiang K, Wan Y, Tang Q. Dapagliflozin protects against chronic heart failure in mice by inhibiting macrophage-mediated inflammation, independent of SGLT2. *Cell Rep Med*. 2023;4:101334. doi: 10.1016/j.xcrm.2023.101334
7. Panico C, Bonora B, Camera A, Chilelli NC, Prato GD, Favacchio G, Grancini V, Resi V, Rondinelli M, Zarra E, et al. Pathophysiological basis of the cardiological benefits of SGLT-2 inhibitors: a narrative review. *Cardiovasc Diabetol*. 2023;22:164. doi: 10.1186/s12933-023-01855-y
8. Chen S, Overberg K, Ghouse Z, Hollmann MW, Weber NC, Coronel R, Zuurbier CJ. Empagliflozin mitigates cardiac hypertrophy through cardiac RSK/NHE-1 inhibition. *Biomed Pharmacother*. 2024;174:116477. doi: 10.1016/j.biopha.2024.116477
9. Billing AM, Kim YC, Gullaksen S, Schrage B, Raabe J, Hutzfeldt A, Demir F, Kovalenko E, Lasse M, Dugourd A, et al. Metabolic communication by SGLT2 inhibition. *Circulation*. 2024;149:860–884. doi: 10.1161/CIRCULATIONAHA.123.065517
10. Rodolico D, Schiattarella GG, Taegtmeyer H. The lure of cardiac metabolism in the diagnosis, prevention, and treatment of heart failure. *JACC Heart Fail*. 2023;11:637–645. doi: 10.1016/j.jchf.2023.02.007
11. Santos-Gallego CG, Vargas-Delgado AP, Requena-Ibanez JA, Garcia-Ropero A, Mancini D, Pinney S, Macaluso F, Sartori S, Roque M, Sabatel-Perez F, et al. Randomized trial of empagliflozin in nondiabetic patients with heart failure and reduced ejection fraction. *J Am Coll Cardiol*. 2021;77:243–255. doi: 10.1016/j.jacc.2020.11.008
12. Santos-Gallego CG, Requena-Ibanez JA, San AR, Ishikawa K, Watanabe S, Picatoste B, Flores E, Garcia-Ropero A, Sanz J, Hajjar RJ, et al. Empagliflozin ameliorates adverse left ventricular remodeling in nondiabetic heart failure by enhancing myocardial energetics. *J Am Coll Cardiol*. 2019;73:1931–1944. doi: 10.1016/j.jacc.2019.01.056
13. Withaar C, Lam C, Schiattarella GG, de Boer RA, Meems L. Heart failure with preserved ejection fraction in humans and mice: embracing clinical complexity in mouse models. *Eur Heart J*. 2021;42:4420–4430. doi: 10.1093/eurheartj/ehab389
14. Schiattarella GG, Altamirano F, Tong D, French KM, Villalobos E, Kim SY, Luo X, Jiang N, May HI, Wang ZV, et al. Nitrosative stress drives heart failure with preserved ejection fraction. *Nature*. 2019;568:351–356. doi: 10.1038/s41586-019-1100-z
15. Shao Q, Meng L, Lee S, Tse G, Gong M, Zhang Z, Zhao J, Zhao Y, Li G, Liu T. Empagliflozin, a sodium glucose co-transporter-2 inhibitor, alleviates atrial remodeling and improves mitochondrial function in high-fat diet/streptozotocin-induced diabetic rats. *Cardiovasc Diabetol*. 2019;18:165. doi: 10.1186/s12933-019-0964-4
16. Kopp EL, Deussen DN, Cuomo R, Lorenz R, Roth DM, Mahata SK, Patel HH. Modeling and phenotyping acute and chronic type 2 diabetes mellitus in vitro in rodent heart and skeletal muscle cells. *Cells*. 2023;12:12. doi: 10.3390/cells12242786
17. Rocca C, De Bartolo A, Guzzi R, Crocco MC, Rago V, Romeo N, Perrotta I, De Francesco EM, Muoio MG, Granieri MC, et al. Palmitate-induced cardiac Lipotoxicity is relieved by the redox-active motif of SELENOT through improving mitochondrial function and regulating metabolic state. *Cells*. 2023;12:12. doi: 10.3390/cells12071042
18. Packer M. Role of deranged energy deprivation signaling in the pathogenesis of cardiac and renal disease in states of perceived nutrient overabundance. *Circulation*. 2020;141:2095–2105. doi: 10.1161/CIRCULATIONAHA.119.045561
19. Packer M. Critical reanalysis of the mechanisms underlying the cardiorenal benefits of SGLT2 inhibitors and reaffirmation of the nutrient deprivation signaling/autophagy hypothesis. *Circulation*. 2022;146:1383–1405. doi: 10.1161/CIRCULATIONAHA.122.061732
20. Cowie MR, Fisher M. SGLT2 inhibitors: mechanisms of cardiovascular benefit beyond glycaemic control. *Nat Rev Cardiol*. 2020;17:761–772. doi: 10.1038/s41569-020-0406-8
21. Packer M, Anker SD, Butler J, Filippatos G, Ferreira JP, Pocock SJ, Sattar N, Brueckmann M, Jamal W, Cotton D, et al. Empagliflozin in patients with heart failure, reduced ejection fraction, and volume overload: EMPEROR-reduced trial. *J Am Coll Cardiol*. 2021;77:1381–1392. doi: 10.1016/j.jacc.2021.01.033
22. Packer M, Wilcox CS, Testani JM. Critical analysis of the effects of SGLT2 inhibitors on renal tubular sodium, water and chloride homeostasis and their role in influencing heart failure outcomes. *Circulation*. 2023;148:354–372. doi: 10.1161/CIRCULATIONAHA.123.064346
23. Logeart D, Taille Y, Derumeaux G, Gellen B, Sirol M, Galinier M, Roubille F, Georges JL, Trochu JN, Launay JM, et al. Patterns of left ventricular remodeling post-myocardial infarction, determinants, and outcome. *Clin Res Cardiol*. 2024;113:1670–1681. doi: 10.1007/s00392-023-02331-z

24. Ritterhoff J, Tian R. Metabolic mechanisms in physiological and pathological cardiac hypertrophy: new paradigms and challenges. *Nat Rev Cardiol*. 2023;20:812–829. doi: 10.1038/s41569-023-00887-x
25. Omar M, Jensen J, Ali M, Frederiksen PH, Kistorp C, Videbaek L, Poulsen MK, Tuxen CD, Moller S, Gustafsson F, et al. Associations of empagliflozin with left ventricular volumes, mass, and function in patients with heart failure and reduced ejection fraction: a substudy of the empire HF randomized clinical trial. *JAMA Cardiol*. 2021;6:836–840. doi: 10.1001/jamacardio.2020.6827
26. Lee M, Brooksbank K, Wetherall K, Mangion K, Roditi G, Campbell RT, Berry C, Chong V, Coyle L, Docherty KF, et al. Effect of empagliflozin on left ventricular volumes in patients with type 2 diabetes, or prediabetes, and heart failure with reduced ejection fraction (SUGAR-DM-HF). *Circulation*. 2021;143:516–525. doi: 10.1161/CIRCULATIONAHA.120.052186
27. Connelly KA, Zhang Y, Visram A, Advani A, Batchu SN, Desjardins JF, Thai K, Gilbert RE. Empagliflozin improves diastolic function in a non-diabetic rodent model of heart failure with preserved ejection fraction. *JACC Basic Transl Sci*. 2019;4:27–37. doi: 10.1016/j.jacbts.2018.11.010
28. Storgaard H, Gluud LL, Bennett C, Grondahl MF, Christensen MB, Knop FK, Vilsboll T. Benefits and harms of sodium-glucose co-transporter 2 inhibitors in patients with type 2 diabetes: a systematic review and meta-analysis. *PLoS One*. 2016;11:e0166125. doi: 10.1371/journal.pone.0166125
29. Hahn VS, Knutsdottir H, Luo X, Bedi K, Margulies KB, Haldar SM, Stolina M, Yin J, Khakoo AY, Vaishnav J, et al. Myocardial gene expression signatures in human heart failure with preserved ejection fraction. *Circulation*. 2021;143:120–134. doi: 10.1161/CIRCULATIONAHA.120.050498
30. Zannad F, Ferreira JP, Butler J, Filippatos G, Januzzi JL, Sumin M, Zwick M, Saadati M, Pocock SJ, Sattar N, et al. Effect of empagliflozin on circulating proteomics in heart failure: mechanistic insights into the EMPEROR programme. *Eur Heart J*. 2022;43:4991–5002. doi: 10.1093/eurheartj/ehac495
31. Li L, Xu J, He L, Peng L, Zhong Q, Chen L, Jiang Z. The role of autophagy in cardiac hypertrophy. *Acta Biochim Biophys Sin Shanghai*. 2016;48:491–500. doi: 10.1093/abbs/gmw025
32. Jiang Q, Lu M, Li J, Zhu Z. Ginkgolide B protects cardiomyocytes from angiotensin II-induced hypertrophy via regulation of autophagy through SIRT1-FoxO1. *Cardiovasc Ther*. 2021;2021:5554569. doi: 10.1155/2021/5554569
33. Castaneda D, Gabani M, Choi SK, Nguyen QM, Chen C, Mapara A, Kassan A, Gonzalez AA, Ait-Aissa K, Kassan M. Targeting autophagy in obesity-associated heart disease. *Obesity (Silver Spring)*. 2019;27:1050–1058. doi: 10.1002/oby.22455
34. Li G, Hou N, Liu H, Li J, Deng H, Lan H, Xiong S. Dapagliflozin alleviates high glucose-induced injury of endothelial cells via inducing autophagy. *Clin Exp Pharmacol Physiol*. 2024;51:e13846. doi: 10.1111/1440-1681.13846
35. Jaikumkao K, Promsan S, Thongnak L, Swe MT, Tapanya M, Htun KT, Kothan S, Intachai N, Lungkaphin A. Dapagliflozin ameliorates pancreatic injury and activates kidney autophagy by modulating the AMPK/mTOR signaling pathway in obese rats. *J Cell Physiol*. 2021;236:6424–6440. doi: 10.1002/jcp.30316
36. Korbut AI, Taskaeva IS, Bgatova NP, Muraleva NA, Orlov NB, Dashkin MV, Khotskina AS, Zavyalov EL, Konenkov VI, Klein T, et al. SGLT2 inhibitor empagliflozin and DPP4 inhibitor linagliptin reactivate glomerular autophagy in db/db mice, a model of type 2 diabetes. *Int J Mol Sci*. 2020;21:21. doi: 10.3390/ijms21082987
37. Madonna R, Moscato S, Cufaro MC, Pieragostino D, Mattii L, Del BP, Ghelardoni S, Zucchi R, De Caterina R. Empagliflozin inhibits excessive autophagy through the AMPK/GSK3beta signalling pathway in diabetic cardiomyopathy. *Cardiovasc Res*. 2023;119:1175–1189. doi: 10.1093/cvr/cvad009
38. Zhang L, Zhang H, Xie X, Tie R, Shang X, Zhao Q, Xu J, Jin L, Zhang J, Ye P. Empagliflozin ameliorates diabetic cardiomyopathy via regulated branched-chain amino acid metabolism and mTOR/p-ULK1 signaling pathway-mediated autophagy. *Diabetol Metab Syndr*. 2023;15:93. doi: 10.1186/s13098-023-01061-6
39. Pandey AK, Bhatt DL, Pandey A, Marx N, Cosentino F, Pandey A, Verma S. Mechanisms of benefits of sodium-glucose cotransporter 2 inhibitors in heart failure with preserved ejection fraction. *Eur Heart J*. 2023;44:3640–3651. doi: 10.1093/eurheartj/ehad389
40. Yang L, Liang B, Li J, Zhang X, Chen H, Sun J, Zhang Z. Dapagliflozin alleviates advanced glycation end product induced podocyte injury through AMPK/mTOR mediated autophagy pathway. *Cell Signal*. 2022;90:110206. doi: 10.1016/j.cellsig.2021.110206
41. Li L, Li Q, Huang W, Han Y, Tan H, An M, Xiang Q, Zhou R, Yang L, Cheng Y. Dapagliflozin alleviates hepatic steatosis by restoring autophagy via the AMPK-mTOR pathway. *Front Pharmacol*. 2021;12:589273. doi: 10.3389/fphar.2021.589273
42. Amer RM, Eltokhy AK, Elesawy RO, Barakat AN, Basha E, Eldeeb OS, Aboalsoud A, Elgharabawy NM, Ismail R. The ameliorative effect of empagliflozin in vigabatrin-induced cerebellar/neurobehavioral deficits: targeting mTOR/AMPK/SIRT-1 signaling pathways. *Molecules*. 2022;27:27. doi: 10.3390/molecules27123659
43. Ren C, Sun K, Zhang Y, Hu Y, Hu B, Zhao J, He Z, Ding R, Wang W, Liang C. Sodium-glucose CoTransporter-2 inhibitor empagliflozin ameliorates sunitinib-induced cardiac dysfunction via regulation of AMPK-mTOR signaling pathway-mediated autophagy. *Front Pharmacol*. 2021;12:664181. doi: 10.3389/fphar.2021.664181
44. Koyani CN, Plastira I, Sourij H, Hallstrom S, Schmidt A, Rainer PP, Bugger H, Frank S, Malle E, von Lewinski D. Empagliflozin protects heart from inflammation and energy depletion via AMPK activation. *Pharmacol Res*. 2020;158:104870. doi: 10.1016/j.phrs.2020.104870
45. Cao Y, Vergnes L, Wang YC, Pan C, Chella KK, Moore TM, Rosa-Garrido M, Kimball TH, Zhou Z, Charugundla S, et al. Sex differences in heart mitochondria regulate diastolic dysfunction. *Nat Commun*. 2022;13:3850. doi: 10.1038/s41467-022-31544-5
46. Packer M. SGLT2 inhibitors: role in protective reprogramming of cardiac nutrient transport and metabolism. *Nat Rev Cardiol*. 2023;20:443–462. doi: 10.1038/s41569-022-00824-4